

# The impact of CD160 deficiency on alloreactive CD8 T cell responses and allograft rejection



MARIA-LUISA DEL RIO, TUAN H. NGUYEN, LAURENT TESSON, JEAN-MARIE HESLAN, ALFONSO GUTIERREZ-ADAN, RAUL FERNANDEZ-GONZALEZ, JULIA GUTIERREZ-ARROYO, LEO BUHLER, JOSÉ-ANTONIO PÉREZ-SIMÓN, IGNACIO ANEGON, and JOSÉ-IGNACIO RODRIGUEZ-BARBOSA

LEON, MADRID, AND SEVILLA, SPAIN; NANTES, FRANCE; FRIBOURG, SWITZERLAND

CD160 is a member of the immunoglobulin superfamily with a pattern of expression mainly restricted to cytotoxic cells. To assess the functional relevance of the HVEM/CD160 signaling pathway in allogeneic cytotoxic responses, exon 2 of the CD160 gene was targeted by CRISPR/Cas9 to generate CD160 deficient mice. Next, we evaluated the impact of CD160 deficiency in the course of an alloreactive response. To that aim, parental donor WT (wild-type) or CD160 KO (knock-out) T cells were adoptively transferred into non-irradiated semiallogeneic F1 recipients, in which donor alloreactive CD160 KO CD4 T cells and CD8 T cells clonally expanded less vigorously than in WT T cell counterparts. This differential proliferative response rate at the early phase of T cell expansion influenced the course of CD8 T cell differentiation and the composition of the effector T cell pool that led to a significant decreased of the memory precursor effector cells (MPECs) / short-lived effector cells (SLECs) ratio in CD160 KO CD8 T cells compared to WT CD8 T cells. Despite these differences in T cell proliferation and differentiation, allogeneic MHC class I mismatched (bm1) skin allograft survival in CD160 KO recipients was comparable to that of WT recipients. However, the administration of CTLA-4.Ig showed an enhanced survival trend of bm1 skin allografts in CD160 KO with respect to WT recipients. Finally, CD160 deficient NK cells were as proficient as CD160 WT NK cells in rejecting allogeneic cellular allografts or MHC class I deficient tumor cells. CD160 may represent a CD28 alternative costimulatory molecule for the modulation of allogeneic CD8 T cell responses either in combination with costimulation blockade or by direct targeting of alloreactive CD8 T cells that upregulate CD160 expression in response to alloantigen stimulation. (Translational Research 2022; 239:103–123)

From the Transplantation Immunobiology and Immunotherapy Section, Institute of Molecular Biology, Genomics and Proteomics, University of Leon, Leon, Spain; INSERM UMR 1064, Center for Research in Transplantation and Immunology, Nantes, France; SFR Bonamy, GenoCellEdit Platform, CNRS UMS3556, Nantes, France; Department of Animal Reproduction, National Institute of Agricultural Research (INIA), Madrid, Spain; Section of Medicine, University of Fribourg, Fribourg, Switzerland; Department of Hematology, University Hospital Virgen del Rocío / Institute of Biomedicine (IBIS / CSIC / CIBERONC), Sevilla, Spain; CIBERONC Consortium, Accion Estrategica en Salud, Grant # CB16/12/00480.

Submitted for Publication April 15, 2021; received submitted July 28, 2021; accepted for publication August 21, 2021.

Reprint requests: J. I. Rodríguez-Barbosa, Laboratory of Transplantation Immunobiology and Immunotherapy, Immunology Section, Institute of Molecular Biology, Genomics and Proteomics, University of Leon, 24071 - Leon, Spain, Phone: +34-987-293079 e-mail: [ignacio.barbosa@unileon.es](mailto:ignacio.barbosa@unileon.es). M. L. del Rio, Laboratory of Transplantation Immunobiology and Immunotherapy, Immunology Section, Institute of Molecular Biology, Genomics and Proteomics, University of Leon, 24071 - Leon, Spain e-mail: [m.delrio@unileon.es](mailto:m.delrio@unileon.es).

1931-5244/\$ - see front matter

© 2021 The Author(s). Published by Elsevier Inc. This is an open access article under the CC BY license (<http://creativecommons.org/licenses/by/4.0/>)

<https://doi.org/10.1016/j.trsl.2021.08.006>

**Abbreviations:** APC = Antigen-presenting cells; B6 mice = C57BL/6Jrj strain; BMCs = Bone marrow cells; BTLA = B-and T-lymphocyte attenuator; CD = Cluster of differentiation; CFSE = Carboxyfluorescein succinimidyl ester; CRD = Cysteine rich domain; CRISPR = Clustered regularly interspaced short palindromic repeats; CTLA4.Ig = recombinant fusion protein composed of the extracellular domain of human CTLA-4 bound to immunoglobulin; CTLA-4 = Cytotoxic T-Lymphocyte Antigen 4; DMEM = Dulbecco's modified eagle medium; FCS = Fetal calf serum; F1 (Balb/c × B6) = Hybrid Balb/c (female) × B6 (male); GPI = Glycosylphosphatidylinositol; HVEM = Herpesvirus entry mediator; IFN $\gamma$  = gamma interferon; Ig = Immunoglobulin; IL-7R $\alpha$  = IL-7 receptor alpha; i.p. = intraperitoneal; KLRG-1 = glycoprotein with a C-type lectin domain and one immunoreceptor tyrosine-based inhibitory motif; KO = Knock-out; LIGHT = homologous to lymphotoxin; exhibits inducible expression and competes with HSV glycoprotein D for binding to herpesvirus entry mediator = a receptor expressed on T lymphocytes; mAb = Monoclonal antibody; MFI = Mean fluorescence intensity; MHC = Major histocompatibility complex; MPECs = Memory precursor effector cells; NK = Natural killer; NKT = Natural killer T cells; SD = Standard deviation; SEM = Standard error of the mean; PBS = Phosphate buffer saline; PD-1 = Programmed death 1; PI = Propidium Iodide; pLNs = peripheral lymph nodes; post-Tx = post-transplantation; SLECs = Short-lived effector cells; TCR = T cell receptor; Th = T helper; TNFSF = Tumor Necrosis Factor Superfamily; TNFRSF = Tumor Necrosis Factor Receptor Superfamily; T7EI = T7 endonuclease; WT = Wild type

## AT A Glance Commentary

del Rio M-L, et al

### Background

CD160 is a member of the immunoglobulin (Ig) superfamily that interacts with HVEM (TNFRSF14), a member of the TNFR superfamily. CD160 expression is restricted to lymphoid cells exhibiting a cytotoxic phenotype (CD8 T cells, NKT cells, NK cells and intraepithelial T cells) and the pattern of expression is coincident in humans and mice. CD160 represents a potential target for immune intervention in CD8 T cell-mediated inflammatory diseases.

### Translational Significance

The treatment of episodes of graft rejection needs better therapeutic interventions to prevent CD8 T cell-mediated rejection. We demonstrated that CD160 functions as a CD28 alternative costimulatory molecule that modulates allogeneic CD8 T cell responses that could enhance costimulation blockade in transplantation.

ultimately determine the outcome of the response.<sup>1,2</sup>

All MHC class I binding receptors in murine NK cells are lectin-like molecules of the Ly49 superfamily, being CD160 molecule, an exception to this general rule. CD160 is a member of the immunoglobulin (Ig) superfamily that interacts with Herpesvirus entry mediator (HVEM)(TNFRSF14), a member of the tumor necrosis factor receptor (TNFR) superfamily.<sup>3–8</sup> CD160 presents several protein isoforms that are the result of mRNA alternative splicing of the CD160 gene: 2 GPI-anchored isoforms with or without IgV-like domain devoid of the transmembrane domain and two transmembrane isoforms with or without IgV-like domain. Besides, a soluble isoform of CD160 (IgV extracellular domain) can be released from the cell membrane by a metalloprotease.<sup>9</sup> *In vitro* soluble CD160 seems to compete with CD8 coreceptor for binding to the alpha 3 domain of MHC class I impairing MHC class I-restricted cytotoxic CD8 T cell responses.<sup>7</sup>

The major isoform of CD160 found in immune cells is the Glycosylphosphatidylinositol (GPI)-anchored membrane glycoprotein that exhibits an IgV-like domain within the extracellular region with six conserved cysteine residues.<sup>7</sup> Although this configuration is suggestive at first sight of potential disulphide bond formation and molecular trimerization,<sup>5,10</sup> the crystal structure of HVEM (TNFRSF14) bound to CD160, favors the notion of a monomeric interaction between CD160 and HVEM.<sup>11,12</sup>

CD160 expression is restricted to lymphoid cells exhibiting a cytotoxic phenotype (CD8 T cells, NKT cells, NK cells and intraepithelial T cells) and the pattern of expression is similar in mice and humans.<sup>5,13,14</sup> Most current evidence pointed to a costimulatory functional role of CD160 in distinct *in vitro* and *in vivo* experimental settings.<sup>6,7,8,15,16</sup> Thus, the engagement of CD160 expressed on human Natural killer (NK) cells by soluble HVEM.Ig costimulates NK cell

## INTRODUCTION

T cell receptor (TCR) recognition of foreign peptide in the context of Major histocompatibility complex self-(MHC) represents the initial trigger of T cell activation that is subsequently modulated during T cell clonal expansion and differentiation toward effector T cells by the intervention of co-stimulatory (positive) and co-inhibitory (negative) signals. These co-signals,

cytotoxicity and gamma interferon (IFN- $\gamma$ ) production.<sup>17</sup> Another example in the same direction is that antibody-mediated triggering of CD160 delivers costimulatory and survival signals to human CD8<sup>bright+</sup> cytotoxic effector T lymphocytes lacking CD28 expression.<sup>18</sup> Cross-linking of CD160 by HLA-C costimulates CD8<sup>+</sup> T cells and activates NK cell cytotoxicity and cytokine production.<sup>8,19,20</sup> In turn, the engagement of HVEM by either CD160, BTLA, or LIGHT enhances Ag-induced T cell proliferation and cytokine production.<sup>21</sup>

As a ligand, CD160 in innate intraepithelial lymphocytes can engage HVEM in epithelial cells of the gut inducing the release of defensins that protect the host against infection.<sup>22</sup> Furthermore, CD160 deficient effector CD8 T cells are impaired to a certain extent in the clearance of some pathogens during infection.<sup>16,22-24</sup> Despite this compelling evidence in favor of the notion that CD160 functions as a costimulatory receptor, a co-inhibitory function has also been assigned to a subset of human CD4 T cells and mouse NKT cells.<sup>25,26</sup> Finally, NK cell-mediated rejection of MHC class I deficient tumor cells was impaired in CD160 Knock-out (KO) mice due to a functional defect associated with a decreased secretion of IFN- $\gamma$  by NK cells.<sup>27</sup>

We previously demonstrated that CD160 is a potential target for immune therapeutic intervention in transplantation.<sup>14</sup> To analyze the intrinsic role of CD160 in the function of allogeneic CD8 T cell cytotoxic responses and NK cell-mediated responses in the context of allograft transplantation and syngeneic tumor rejection, we took advantage of CRISPR (clustered regularly interspaced short palindromic repeats) / Cas9 technology (CRISPR/Cas9) for the generation of CD160-deficient mice. This technology permits the generation of targeted mutations into the genome of many species with unprecedented efficiency.<sup>28-32</sup> To that end, exon 2 encoding the signal peptide of CD160 gene was targeted to introduce a genetic modification that led to the formation of several premature stop codons with the subsequent truncation of protein expression. Herein, using an adoptive transfer model of parental B6 lymphocytes into semiallogeneic F1 recipients (graft vs host reaction), we demonstrated that CD160 deficiency delays alloreactive CD4 T cells and CD8 T cell proliferation at the initial phase of T cell clonal expansion (from day 1 – day 3) when compared to the rate of proliferation of Wild type (WT) T cells. This defective clonal expansion altered CD8 T cell differentiation leading to a change in the composition of the effector T cell pool that resulted in the alteration of the MPECs/SLECs ratio. However, these deficits were not translated into a detectable significant impairment of graft rejection across an MHC class I mismatched barrier, although CTLA4.Ig co-stimulation

blockade showed an enhanced survival tendency that did not reach statistical significance. Finally, we found no evidence that CD160 could affect NK-cell mediated rejection of fully MHC mismatched cellular allografts or MHC class I deficient tumor cells.

## MATERIAL AND METHODS

**Rodents.** Female mice of mixed background (CBA  $\times$  C57BL/6JRj) F1 (7–8 weeks old) were superovulated by intraperitoneal injections of 5 IU of pregnant mare serum gonadotropin (PMSG, Folligon, MSD Animal Health) and an equivalent dose of human chorionic gonadotropin (hCG, Sigma) was injected every 2 days. Superovulated female mice were mated with C57BL/6JRj males and zygotes were recovered from oviduct.<sup>33</sup> CD160 deficient mice were then backcrossed for more than 15 generations onto C57BL/6JRj background (herein referred as B6 mice) at the animal facility of the University of Leon (Spain). B6 mice were purchased from Janvier (France). Eight to twelve-week-old female CB6F1 mice (Balb/c  $\times$  B6), Balb/c mice, and B6.C-H2-K<sup>bm1</sup>/ByJ (bm1) mice were bred at the animal facility of the University of Leon and were used in our experiments. All animals were maintained with a 12-hour dark-light cycle at 22 °C temperature and received ad libitum food and water. All experiments with rodents were performed following animal protocols approved by the Animal Welfare Committee of the University of Leon # ULE-011-2020 and followed the European Guidelines for Animal Care and Use of Laboratory Animals.

**CRISPR/Cas9 genome targeting strategy for knocking-out CD160 gene expression.** The sequence encoding exon 2 of the CD160 gene was introduced into the optimized CRISPR design tool CHOPCHOP website (<https://chopchop.cbu.uib.no/>) for the generation of the oligo guides. A set of 5 different single-stranded oligodeoxynucleotide (ssODN) guides (sense and antisense) was chosen from a list of predicted sequences based on the observed score and were synthesized by IDT (Coralville, IA, USA). The sequences of oligonucleotides used in this study are listed in **Table I**.

The pX330-U6-Chimeric\_BB-CBh-hSpCas9 plasmid (Addgene plasmid # 42230) was digested with *BbsI* restriction enzyme and the linearized vector was dephosphorylated using alkaline phosphatase (Thermo Fisher Scientific) and was then purified from a 1% low melting point agarose gel. The set of the five different pairs of oligo DNA targeting exon 2 were synthesized, annealed, phosphorylated and ligated into *BbsI*-digested site of the above-mentioned bicistronic expression vector containing Cas9.<sup>34,31</sup>

**In vitro testing of genome editing with T7EI endonuclease.** These genetic constructs were cloned

**Table I.** List of designed ssODN oligo guides and their sequence used for targeting exon 2 of CD160 gene

Seq Name	Sequence with PAM site in red
mCD160-1 sgRNA (-)	CACGGAAATGTTGACTTTGC TGG
mCD160-2 sgRNA (-)	AGCTTTGGCCAGGGGCCATC AGG
mCD160-3 sgRNA (+)	GCAATTGTGAACCTCCAACA TGG
mCD160-4 sgRNA (-)	GGAAGTTCACAATTGCCAGC AGG
mCD160-5 sgRNA (-)	GGGCACAGCAGCTTTGGCCA GGG

into a plasmid pX330 containing each oligo DNA guide along with Cas9 and then transfected into murine Hepa 1-6 hepatocyte cell line grown in Dulbecco's modified Eagle medium (DMEM) plus 10% Fetal Bovine Serum, 2 mM glutamine, 1 mM sodium pyruvate and penicillin/streptomycin. Cells were seeded in 24-well plates and transfected with lipofectamine 2000 (Life Technologies, NY, USA) complexed to 2  $\mu$ g per well of pX330 plasmid co-expressing Cas9 along with each oligo DNA guide targeting exon 2 of mouse CD160, following the manufacturer's instructions. Three days after transfection, genomic DNA was extracted from transiently transfected cells (NucleoSpin Tissue kit Macherey Nagel, Germany) and was quantified using the NanoDrop 2000 spectrophotometer (Thermo Fisher Scientific, Illkirch, France). The A260/A280 ratio was calculated to monitor the quantity and quality of the extracted genomic DNA. Indel mutational activity of each targeting vector was determined using the T7EI mismatch detection assay.<sup>35</sup> Flanking sense and antisense primers of CD160 exon 2 were used for PCR amplification of genomic DNA extracted from the transfected cells using Herculase II fusion polymerase (Table II). An amplicon of 616 bp product was denatured and slowly re-annealed (95°C, 2 minutes; 95°C to 85°C, -2°C/S; 85°C – 25°C, -1°C/S) to generate homoduplex/heteroduplex mix. This DNA product was then digested in the presence of 5U of T7EI restriction enzyme (New England Biolabs) at 37°C for 30 minutes. Digested DNA fragments were run into a 2% agarose gel. The ratio of cleaved to uncleaved products was used to calculate non-homologous end joining (NHEJ) frequency as previously described using Image J software. NHEJ frequency was determined as follows: % gene modification =  $100 \times (1 - (1 - \text{fraction cleaved})^{1/2})$ .

**In vitro transcribed sgRNA and Cas9 mRNA.** For the generation of sgRNA of the selected targeting guide, T7 promoter sequence was appended to ssODN guide (sgRNA CD160-4) by PCR amplification from the template pX330-Cas9-sgRNA, in which the guide was

**Table II.** Sequence of PCR primers flanking exon 2 for the amplification of the mutated CD160 gene

Name	Sequence	PCR amplicon
rUpTE71-sgmCD160	Acacgggcta ttcaccaaag	616 bp
rLoTE71-sgmCD160	Taccttcccc tcacaactg	

previously cloned. The PCR amplicon was purified using NucleoSpin Gel and PCR Clean-up (Macherey Nagel, Germany). This amplicon was then used as the template for *in vitro* transcription following the instructions of MEGAShortscript T7 kit (Invitrogen Life Technologies) and the transcribed T7-sgRNA was treated with DNase I.

The Cas9 mRNA was transcribed using *PmeI*-digested Cas9 expression JDS246 plasmid (Addgene plasmid # 43861) and the mMACHINE T7 ULTRA Transcription Kit (Invitrogen Life Technologies). Once the transcribed mRNA for Cas9 was obtained, a poly(A) tail was added and the contaminating DNA was removed from the reaction with DNase I. Both Cas9 mRNA and the T7-promoter appended to the RNA-guide were purified using MEGAclean kit (Invitrogen, Life Technologies).

**Generation and screening of the offspring for the selection of a CD160 deficient mouse line.** A mixture of 100 ng/mL of Cas9 mRNA and 40 ng/mL of sgRNA was microinjected into the cytoplasm of zygotes (3–5 pl) using a Piezo impact-driven micromanipulator (Prime Tech Ltd., Ibaraki, Japan).<sup>36</sup> After microinjection, zygotes were cultured in potassium simplex optimized medium (KSOM, Sigma) in a humidified atmosphere of 5% CO<sub>2</sub> and 95% air at 37°C. Microinjected embryos were transferred into the uterus of pseudo-pregnant females at the 2-cell or blastocyst stage.<sup>37</sup> CD160 deficient mice were backcrossed for 15 generations into B6 genetic background and the screening of the offspring was performed using the primers described in Table III.

**Flow cytometry analysis of CD160 expression in primary and secondary lymphoid organs.** The following list of antibodies was used for the staining of immune cells from primary and secondary lymphoid organs (Table IV). All antibodies in this study were titrated to determine the optimal dilution to stain  $0.5-1 \times 10^6$  cells per tube. Fc receptors were blocked by pre-incubating cell suspensions with 2  $\mu$ g/mL of blocking anti-Fc $\gamma$ R mAb (clone 2.4G2) that was produced and purified in-house. This antibody was used to reduce non-specific binding to Fc receptors before adding biotinylated- or fluorochrome-labeled mAbs.<sup>38</sup> Biotinylated antibodies were detected with Streptavidin (SA)-PE, SA-PE-Cy7,

**Table III.** Screening of the offspring to select CD160 KO mice during the backcrossing into B6 genetic background

Name	Sequence	PCR amplicon
PCR2KO1F	Gcagccacag accagcaaag	KO: 303 bp
rLoTE71-sgmCD160	Tacctccccctc acaactg	WT: 350 bp

or SA-Brilliant Violet 421. Dead cells and debris were excluded from acquisition by propidium iodide (PI). Flow cytometry acquisition was carried out on Aurora Cytex spectral cytometer (Cytex Biosciences) and data analysis was performed using FlowJo VX10.

Splenocytes and bone marrow cell suspensions were stained with anti-CD3, anti-DX5, and anti-CD160 antibodies to differentiate NK cells, NKT cells, CD3 T cells. CD8 T cells were also stained in combination with anti-CD62L and anti-CD44 antibodies to differentiate T central memory (TCM, CD62L<sup>+</sup> CD44<sup>+</sup>) from T effector memory (TEM, CD62L<sup>-</sup> CD44<sup>+</sup>) or naïve T cells (CD62L<sup>-</sup> CD44<sup>-</sup>) under steady-state conditions. Finally, CD160 expression was also evaluated in single-positive (CD4SP, CD8SP) and CD4/CD8 double-positive thymocytes.

**CFSE-labeling of donor alloreactive T cells for monitoring the early phase of T cell clonal expansion.** In this experimental setting, parental donor T cells are weakly resisted by host F1 NK cells (hybrid resistance)

and this barrier can be overcome by the infusion of a large number of donor semiallogeneic splenocytes.<sup>39,40</sup>  $50 \times 10^6$  of parental B6 lymphocytes (splenocytes plus peripheral lymph nodes) per mL were resuspended in endotoxin-free D-PBS and were labeled with 5  $\mu$ M carboxy-fluorescein diacetate succinimidyl ester (CFDASE; Molecular Probes, Inc., Eugene, OR) with intermittent gently mixing for 12 minutes at 37° C. Unbound CFSE was quenched by the addition of 10 ml of complete medium containing 10% of Fetal calf serum (FCS) followed by 2 washes in endotoxin-free D-PBS.<sup>41</sup>  $90 \times 10^6$  of Carboxyfluorescein succinimidyl ester (CFSE)-labeled parental lymphocytes from B6 WT or CD160 KO were adoptively transferred into non-irradiated F1 (CB6F1) recipients and the initial phase of T cell activation and clonal expansion was followed up to day 3 and 8 cycles of T cell division were monitored.<sup>42</sup>

For the measurement of the alloreactive response, we took advantage of method 3 described by Suchin et al., which calculates the recovered precursor frequency of alloreactive CD4 T cells and CD8 T cells taking into account the number of cells homing to the spleen 24 hours after the cell transfer. This recovered precursor frequency is equal to the absolute number of dividing CD4 T cells or CD8 T cells at day 3 after the adoptive transfer divided by the absolute number of CFSE-labeled CD4 T cells or CD8 T cells in the spleen 24 hours after the adoptive transfer (immediately before the onset of clonal expansion).<sup>42</sup> This approach

**Table IV.** List of antibodies used in this work

Receptor	Label	Clone	Company
CD3	AF-488	145-2C11	Biologend (#100321)
CD160	Biotin	6H8	14
CD270 (HVEM)	Bio	5B7	65
CD272 (BTLA)	Bio	4G12b	44
CD49b	APC	DX5	Biologend, #108910
CD4	PE-Cy7	GK1.5	Biologend, # 100422
CD4	APC	GK1.5	Beckton Dickinson, #553051
CD8	PE-Cy7	53-6.7	Biologend, # 100721
CD8	APC	53-6.7	Biologend, # 100712
CD19	PE	6D5	Biologend, # 115507
CD62L	AF-647	MEL-14	Biologend, #104421
CD44	PE-Cy7	IM7	Biologend, #103030
CD127 (IL7-R $\alpha$ )	PE	SB/199	Biologend, #121111
KLRG-1	Bio	MAFA	Biologend, #138406
CD27	Bio	LG.3A10	Biologend, #124205
CD69	Bio	H1.2F3	Beckton Dickinson, #553235
CD69	APC	H1.2F3	Biologend, #104513
CD137 (4-1BB)	Bio	17B5	Thermofisher, #16-1371-85
K <sup>d</sup>	FITC	SF1-1.1	Biologend, #116606
K <sup>b</sup>	AF-647	AF6-88.5	Biologend, # 116512
Rat IgG2a Isotype control	Bio	AFRC MAC 157	72
Mouse IgG2b Isotype control	Bio	MCP-11	14

considers both proliferation and cell engraftment, because not all alloreactive donor cells adoptively transferred managed to home and settle in the spleen due to the lack of space or functional niches.

To follow the course of T cell differentiation towards effector T cells from day 3 onwards,  $90 \times 10^6$  of donor WT or CD160 KO lymphocytes were adoptively transferred to CB6F1 recipients. The donor anti-host alloreactive response (graft vs host reaction) was measured overtime by staining 2 sets of surface molecules expressed on donor and host CD4 T cells and CD8 T cells. Set 1 comprised molecules of the HVEM/BTLA/CD160 pathway and set 2 encompassed T cell-related differentiation molecules: IL-7R $\alpha$ , KLRG-1, CD27, and CD69.

**Allogeneic skin grafting across an MHC class I mismatched barrier.** Abatacept (human recombinant CTLA-4.Ig, Bristol-Myers Squibb) or irrelevant human IgG1 control were administered intraperitoneal (i.p.) at day 0 (1 mg), day 7 (0.5 mg), and day 14 (0.25 mg) to recipient B6 WT and CD160 KO mice that were grafted with allogeneic bm1 tail skin under deep anesthesia, following a general procedure previously reported.<sup>43</sup> Briefly, bm1 skin grafts were placed on the right lateral side of the thorax of B6 recipient mice under ketamine-xylazine anesthesia and then covered with terramycin ointment impregnated gauze. The bandage was removed on day 8 post-transplantation (post-Tx). Signs of onset and progression of rejection, such as dryness, loss of hair, contraction, scaling, and necrosis were examined by visual inspection every other day and data were recorded for 60 days. Skin grafts were considered fully rejected when complete necrosis of the skin graft was observed or less than 10% of the original size of the skin graft was still present.

**Cellular allograft transplantation and RMA/RMA-S mouse tumor model to monitor NK cell-mediated rejection.** For the cellular allograft model,  $15 \times 10^6$  of syngeneic B6 cells and allogeneic Balb/c cells were labeled with 1  $\mu$ M and 0.25  $\mu$ M of CFSE respectively, mixed at a 1:1 ratio and injected intravenously. The kinetics of graft rejection was monitored at 21, 42 and 70 hours. The percentage of specific lysis of the allogeneic population was calculated following an equation described previously: % specific lysis:  $100 - [(\text{percentage of target population in experimental} / \text{percentage of syngeneic population in experimental}) \times 100]$ .<sup>44</sup>

On the other hand,  $1 \times 10^6$  of differentially CFSE-labeled syngeneic RMA (10  $\mu$ M CFSE, MHC sufficient) and RMA-S (2.5  $\mu$ M CFSE, MHC deficient) leukemia tumor cells were mixed at a 1:1 ratio and injected i.p. with a 30 G needle.<sup>45</sup> Twenty-four hours later, the peritoneal cavity was washed with 8 ml of EDTA/Glucose/PBS buffer for 2 minutes and the

immune cells were harvested and analyzed by flow cytometry. The absolute number of cells (tumor cells plus host immune cells) extracted from the peritoneal cavity was calculated according to the volume recovered and then the total cell counts were normalized to the volume injected.

**Statistical analysis.** Collected data were organized in Excel worksheets and in GraphPad Prism 7.00 tables and plots (Graph Pad Software Inc, La Jolla, CA). For the statistical analysis of normally distributed data, statistical significance was calculated using multiple Student *t*-test one per row (time points) and column groups (donor WT vs host F1 and donor CD160 KO vs host F1) corrected for multiple comparisons using the Holm-Sidak method. These statistical studies were performed under the conditions of independence of the data, normality test (Kolmogorov test) and equal variances among groups (Bartlett's test).

Skin graft survival was calculated by using the Kaplan–Meier life table method and statistical analysis for the comparison of the survival curves was performed by the log-rank (Mantel-Cox) test. A value of  $P < 0.05$  was considered statistically significant.

## RESULTS

**CRISPR/Cas9 gene targeting approach for the generation of CD160-deficient mice.** Aceview analysis of the gene-encoding mouse CD160 suggests a complex locus that maps on chromosome 3 and appears to produce several protein isoforms with no sequence overlap. The scheme of supplementary figure 1A shows the genomic organization of CD160 gene encoded by five exons (exon 1: 5UTR, exon 2: end of 5UTR plus signal peptide sequence, exon 3/4: extracellular domain, exon 5: Transmembrane, intracellular domain and 3UTR). Five potential different mRNA alternative variants have been described, of which, 4 were spliced variants and one was an unspliced variant.<sup>46</sup> To elucidate the role of CD160 in the setting of allogeneic transplantation, exon 2 encoding the signal peptide was targeted to introduce indel mutations into CD160 gene aiming at interrupting protein expression (Supplementary Figure 1A) with a plasmid encoding Cas9 and the selected oligo guide (pX330, Addgene) (Supplementary Figure 1B). T7EI mismatched endonuclease assay was performed on genomic DNA extracted from Hepa 1-4 cell line after transfection with the different genetic constructs encoding sgRNA guides and Cas9. The amount of 50 – 100 ng of genomic DNA obtained from transfected cells was subjected to PCR using exon 2 flanking primers and the PCR amplicon was sequenced to characterize the indel mutation that

resulted in a 47 bp deletion (Table II). From this experiment, sgRNA-CD160-4 was chosen for targeting exon 2 of CD160 due to its optimal cleavage efficiency of the heteroduplex mix in the T7EI endonuclease assay (Supplementary Figure 1C).

The CRISPR/Cas9 strategy to target exon 2 resulted in a deletion of 46 bp at the end of exon 2 plus 1 bp deletion that corresponded to the first base of exon 3 (Supplementary Figure 2A). The consequence of this mutation was the introduction of several premature stop codons within exon 3 and the subsequent inactivation of all possible isoforms of CD160 (Supplementary Figure 2B). For the selection of the colony founders, total genomic DNA was isolated from the tail or ear of each newborn a week after birth, and PCR amplified by using primers flanking exon 2/3 mutation. The PCR amplicon obtained gave the following pattern of bands: WT, 350 bp band; CD160 KO, 303 bp band and CD160<sup>+/-</sup>, 350 bp and 303 bp bands (Table III, Fig 2C). The CD160 deficient mouse line was then back-crossed into B6 genetic background for 15 generations to dilute out any potential off-target effect. At the end of the backcrossing process, CD160 KO mice were challenged with syngeneic B6 skin grafts to confirm genetic identity and subsequent indefinite graft survival.

**A deletion of 47 bp affecting exon 2/3 led to inactivation of CD160 expression on lymphoid cells.** The

pattern of CD160 expression is restricted to cytotoxic cells of lymphoid organs under steady-state conditions.<sup>13,14</sup> Cell suspensions of primary lymphoid organs (thymus and bone marrow) and spleen were prepared to validate that the chosen targeting strategy achieved the complete abrogation of CD160 protein expression. Cells suspensions were then stained with anti-DX5, anti-CD3, and anti-CD160 (clone 6H8, rat IgG2<sub>b</sub>, k) antibodies and analyzed by flow cytometry applying the following gates: NK cells (DX5<sup>+</sup> CD3<sup>-</sup>), NKT cells (DX5<sup>+</sup> CD3<sup>+</sup>), and CD3 T cells (DX5<sup>-</sup> CD3<sup>+</sup>). Under non-inflammatory conditions, CD160 expression was detected in half of the NKT cells, but was barely present on NK cells and T cells of the spleen (Fig 1A). Most NKT cells in the bone marrow resulted positive for CD160 whereas the expression of CD160 in NK cells and T cells was rather weak, although more pronounced than that observed in the spleen of similar cell subtypes (Fig 1A/B).

CD160 protein expression was also detected in a subset of CD8 T cells of the bone marrow and to a lesser extent was evidenced in CD4 T cells in the same hematopoietic compartment (Fig 1B). There was no detectable expression of CD160 on B cells from bone marrow or spleen (data not shown). Since a small population of CD8 memory-type T cells has been shown to express constitutively CD160,<sup>13,14</sup> we next determined CD160 expression on different cell populations

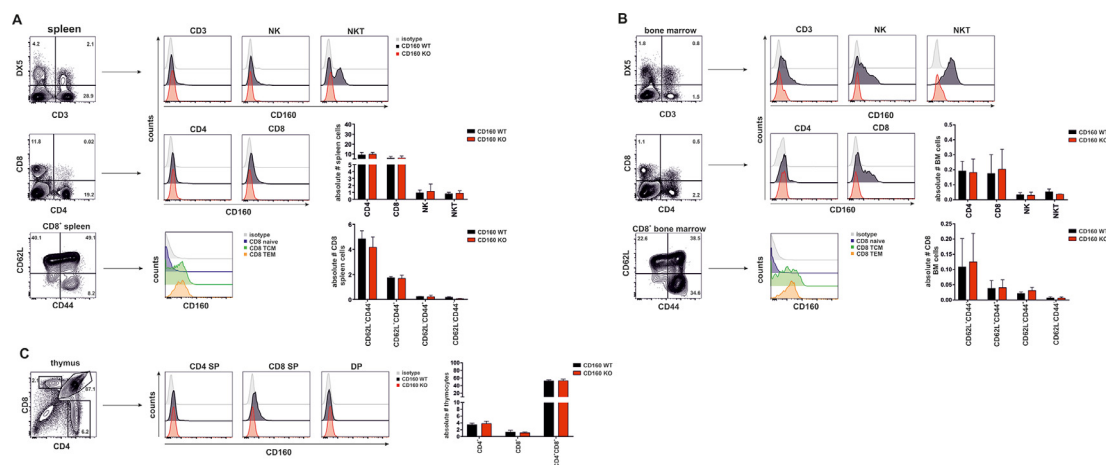


**Fig 1.** Lack of CD160 expression in spleen, bone marrow, and thymus of CD160 deficient mice. (A – B) Histograms showing CD160 expression in CD3 T cells, NK cells and NKT cells of spleen and bone marrow of WT and CD160 KO mice and the absolute number of T cell subsets (CD4 T cells and CD8 T cells), NKT cells, NK cells in these hematopoietic compartments. Gated CD8 T cells from spleen and bone marrow cell suspensions of CD160 WT and CD160 KO mice were further analyzed for CD160 expression using CD44 and CD62L surface markers. TCM: T central memory and TEM: T effector memory. (C) CD4 and CD8 single-positive (SP) thymocytes and CD4 and CD8 double-positive (DP) thymocytes were stained with anti-CD160 antibody and the absolute number of these cell types were also analyzed. CD160 expression was detected using a biotinylated rat anti-mouse CD160 mAb (clone 6H8) followed by incubation with streptavidin-BV421. The plotted data represent the mean±SD from 5 mice per group. NK, Natural killer; NKT, Natural killer T cells; KO, Knock-out. For interpretation of the references to color in this figure legend, the reader is referred to the Web version of this article.

classified based on CD62L and CD44 expression markers. T cell central memory (CD62L<sup>+</sup> CD44<sup>+</sup>) or T cell effector memory (CD62L<sup>-</sup> CD44<sup>+</sup>) populations expressed CD160 on their cell membrane in the spleen and bone marrow compartments (Fig 1A/B).

CD160 expression on thymocytes showed a fluorescent shift in the staining of CD8 single-positive T cells that suggests a weak expression on this cell subset whereas no expression was detectable on CD4 single positive cells or double-positive thymocytes (Fig 1C).

As expected, there was no detectable expression of CD160 on spleen, bone marrow, and thymus of CD160 deficient mice, confirming the lack of protein expression on the cell membrane of immune cells of these hematopoietic compartments (Fig 1A – C). In agreement with a previous report, NKT cells, NK cells, and T cells seem to develop normally in CD160 deficient mice as in WT mice, since no statistically significant differences were found (Fig 1A/B/C).<sup>27</sup>

These data confirm a complete abrogation of CD160 expression in lymphoid cells of different hematopoietic compartments of primary and secondary lymphoid organs of CD160 deficient mice, in which exon 2 was targeted by CRISPR/Cas9.

**Normal upregulation of CD69 and CD137 expression on CD160 deficient CD8 T cells or NK cells in response to IL-2.** It has been previously shown that NK cells stimulated with increasing concentrations of IL-2 upregulate the expression of CD160 in an IL-2 dose-dependent manner.<sup>27</sup> To evaluate the effect of IL-2 in NK cell and CD8 T cell activation, splenocytes from WT or CD160 KO mice were exposed *in vitro* to IL-2 (5000 units/mL) for 48 hours and the co-expression of CD137 and CD69 was measured by flow cytometry. As seen in Fig 2, WT and CD160 KO CD8 T cells and NK cells responded to the same extent *in vitro* to IL-2 or IL-2 plus anti-NK1.1 antibody leading to rapid and comparable upregulation of both surface markers CD137 and CD69, and no statistically significant differences between CD160 WT and CD160 deficient mice were found.

The lack of CD160 expression did not compromise the activation of either NK cells or CD8 T cells in response to IL-2 cytokine stimulus.

**CD160 deficiency delayed early T cell clonal expansion.** As CD160 expression is upregulated upon T cell activation in response to conventional antigens or polyclonal stimuli, we evaluated the frequency of T cells responding against alloantigens *in vivo*. CFSE-labeled parental splenocytes and lymph node cells were adoptively transferred into non-irradiated F1 semiallogeneic recipients. Each time a parental T cell divides, the CFSE fluorescence intensity present in the

daughter cells halves sequentially.<sup>41</sup> This permits the resolution of up to 8 generations of daughter cells within the alloreactive CD4 T cell and CD8 T cell populations dividing during the first 72 hours. Parental donor T cells become activated after the adoptive transfer into F1 recipients in response to H-2<sup>d</sup> mismatched alloantigens present in the APC of the host F1 (direct antigen presentation). The participation of the indirect pathway of antigen presentation is transient, as this pathway is abrogated gradually due to donor alloreactive T cell targeting of the host hematopoietic compartment. When this approach is combined with fluorochrome-conjugated antibody staining of surface molecules, the phenotypical changes in expression as cells divide can be monitored.<sup>42,47</sup>

To elucidate whether CD160 deficiency could influence the early events of the alloreactive T cell proliferative response, unfractionated parental splenocytes, and lymph nodes from B6 WT or CD160 deficient donors were CFSE-labeled *ex-vivo* and then adoptively transferred into semiallogeneic F1 recipients. The recovered alloreactive T cell precursor frequency was calculated using the “method 3” described by Suchin et al.<sup>42</sup> This approach accounts for the total number of donor cells that emigrated to the spleen and occupied a niche where they undergo the initial phase of clonal expansion. As shown in Fig 3, the recovered precursor frequency of alloreactive donor CD4 T cells and donor CD8 T cells was significantly greater in WT mice than in CD160 KO mice, meaning that CD160 deficient mice exhibited a compromised early T cell clonal expansion (Fig 3 A – B \*\*,  $P < 0.005$ ). The CD4/CD8 ratio (the absolute number of proliferating CD4 T cells divided by the absolute number of proliferating CD8 T cells) was significantly higher in CD160 KO mice than in WT mice denoting that CD8 T cell proliferation in the former was less active than in the latter (Fig 3C, \*,  $P < 0.05$ ).

Overall, these data suggest that CD160 expression on T cells is required during the initial phase of T cell clonal expansion on both alloreactive donor CD4 T cells and donor CD8 T cells.

**The process of T cell differentiation toward effector T cells is associated with changes in HVEM, BTLA and CD160 expression.** We next studied the influence of the T cell differentiation process in the pattern of HVEM, BTLA, and CD160 expression on alloreactive T cells and evaluated whether CD160 deficiency could modulate the level of expression of the partner molecules of the pathway. To that aim, we compared the baseline expression levels of these molecules in recipient F1 host T cells with those present in alloreactive donor CD4 T cells and donor CD8 T cells of WT and CD160 KO along the course of the allogeneic immune response, as shown in Fig 4. HVEM, the



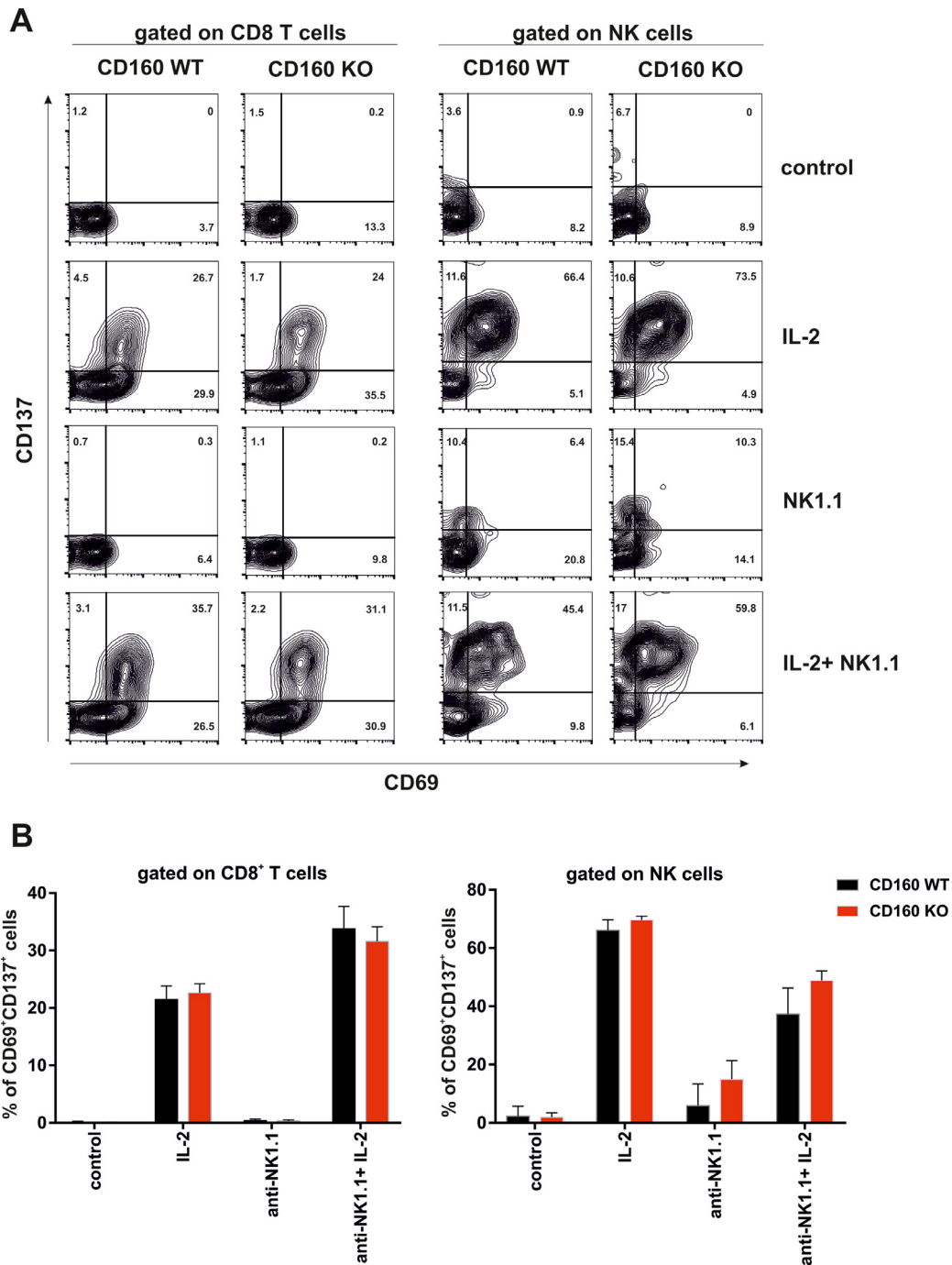


**Fig 2.** NK cells and CD8 T cells respond similarly to IL-2 by upregulating CD69 and CD137. (A) Splenocytes from wild-type or CD160 deficient mice were incubated with PBS, IL-2, bound to plate anti-NK1.1 antibody or a mixture of IL-2 plus anti-NK1.1 antibody. Representative density plots illustrating the combined expression of CD137 and CD69 markers are shown at 48 hours after stimulation to determine the activation status of cytotoxic cells. No significant differences in expression of these markers were found when wild-type were compared to CD160 deficient cells. Each quadrant indicates the percentage of each cell population. One representative experiment out of 3 is depicted. (B) The percentage of CD8 T cells and NK cells that were double positive CD69<sup>+</sup>/CD137<sup>+</sup> were analyzed after exposure to either anti-NK1.1 antibody and/or recombinant IL-2. These data come from a pool of three independent experiments with similar results and expressed as mean±SD. NK, Natural killer; PBS, Phosphate buffer saline. For interpretation of the references to color in this figure legend, the reader is referred to the Web version of this article.

shared partner molecule of BTLA and CD160, displayed a mean fluorescence intensity (MFI) that decreased slightly upon T cell activation in alloreactive donor T cells and then recovered its expression slowly during the course of the allogeneic response approaching HVEM baseline levels of host F1 T cells at the end of the response, once the alloantigen in the hematopoietic host compartment had been extensively eliminated (Fig 4A – B, right lower panel). In contrast, B- and T-lymphocyte attenuator (BTLA) followed an inverse pattern of expression to HVEM and showed a significant and rapid increase after T cell activation in alloreactive donor CD4 T cells and donor CD8 T cells of WT and KO mice and, then, gradually declined from day 3, reaching baseline expression level similar to that of T cells of F1 host at day 12. These changes in BTLA expression were more prominent in donor CD4 T cells than in donor CD8 T cells (Fig. 4A – B, center lower panel). Regarding CD160

expression, donor alloreactive CD8 T cells increased rapidly its expression remaining significantly higher than that in host F1 CD8 T cell counterparts at all-time points measured (Fig 4B, lower panel). This upregulation in expression of CD160 was much more pronounced in donor CD8 T cells than in donor CD4 T cells of WT and KO mice (Fig 4A – B, left lower panel). As expected, no changes in CD160 expression were observed in donor T cells of CD160 deficient mice. CD160 levels of expression in either donor CD4 T cells or donor CD8 T cells were statistically significantly higher than in counterpart host F1 T cells (Fig 4A – B, left lower panel).

In summary, HVEM and BTLA/CD160 expression are reciprocally regulated. Thus, whereas HVEM expression decreased after T cell activation and then recovers, BTLA and CD160 augmented its expression. BTLA increased its expression transiently while CD160, once upregulated after T cell activation,

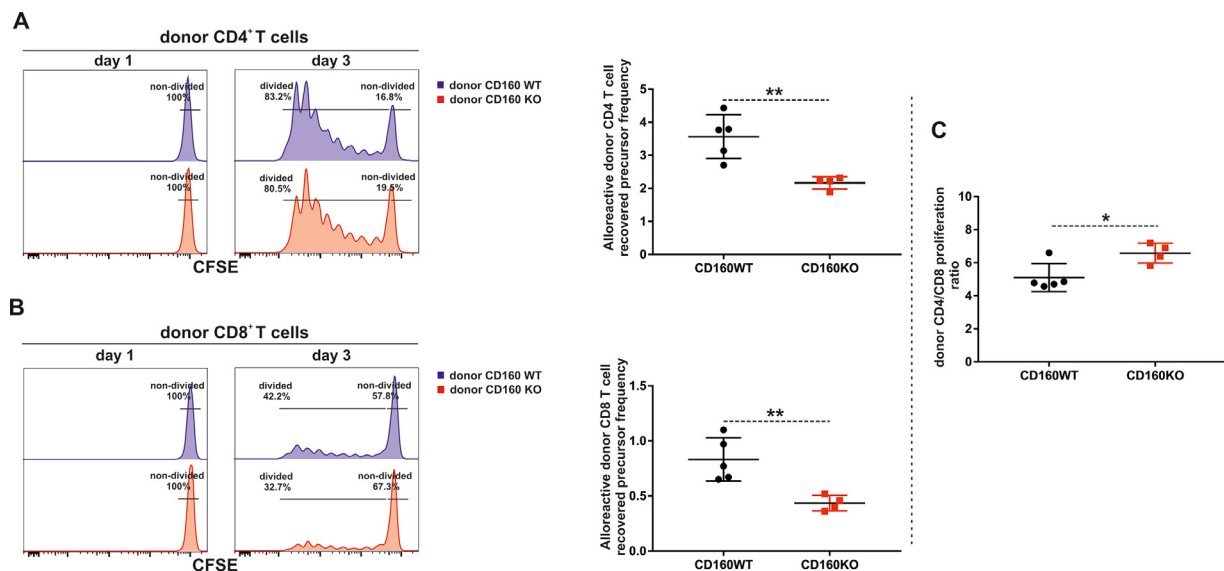


**Fig 3.** Defective alloreactive T cell clonal expansion in the absence of CD160.  $90 \times 10^6$  of CFSE-labeled wild-type or CD160 deficient lymphocytes (splenocytes plus peripheral node lymphocytes) were adoptively transferred into CB6F1 recipients. Donor type allogeneic WT and CD160 KO CD4 T cells (A, left panel) and CD8 T cells (B, left panel) were analyzed by flow cytometry in spleen of host F1 recipients at day 1 or day 3 after the adoptive transfer. The histograms show the percentage of non-divided vs divided donor WT or CD160 KO CD4 T cells and CD8 T cells. The recovered donor alloreactive T cell precursor frequency was calculated for CD4 T cells and CD8 T cells in WT and CD160 KO, following “method 3” described by Suchin et al., as mentioned in material and methods section. The mean  $\pm$  SD of the alloreactive donor CD4 T cells (A, middle panel) and donor CD8 T cells (B, middle panel) recovered precursor frequency was plotted for WT and CD160 KO mice and the statistically significant differences were calculated by applying unpaired Student’s *t* test. (C) The mean  $\pm$  SD of the donor CD4/CD8 ratio (the absolute number of proliferating CD4 T cells divided by the absolute number of proliferating CD8 T cells) was plotted for WT and CD160 KO mice. *p* values were considered statistically significant according to the following criterion: \*, *P* < 0.05; \*\*, *P* < 0.005; \*\*\*, *P* < 0.0005. WT, Wild type; KO, Knock-out. For interpretation of the references to color in this figure legend, the reader is referred to the Web version of this article.

remained highly expressed during the course of the allogeneic response.

**CD160 expression influences the course of T cell differentiation of donor alloreactive CD8 T cells towards effector T cells.** An open question in viral infections is the understanding of the differences between terminal effector CD8 T cells that arise at the peak of clonal expansion phase (effector phase and the subsequent acquisition of cytolytic function). Most effector cells die soon after fighting the infection (short-lived effector cells: SLECs, 95% of total effector cells), whereas some effector cells survive after the contraction phase of the response (memory precursor effector cells: MPECs, 5% of the total effector cells). The latter population ultimately will give rise to long-term memory T cells, once the contraction phase is accomplished. The combined use of killer cell lectin-like receptor G1 (KLRG-1, a glycoprotein with a C-type lectin domain and one immunoreceptor tyrosine-based inhibitory motif) and CD127 (IL-7R $\alpha$ , a receptor for the homeostatic cytokine IL-7) permits the distinction of effector CD8 T subsets in transplantation as well as in the course of viral infection.<sup>48-52</sup>

As T cells clonally expand and divide toward effector T cells, this process of T cell differentiation is more dependent on IL-2 and CD25 (IL-2R $\alpha$ ) expression and less dependent on IL-7. At the effector phase of the response, T cells that have acquired cytotoxic function tackle and clear the stimulus that triggers the response and become more dependent on IL-7 to survive as memory T cells. The T cell differentiation process towards effector cells is associated with an increase in the percentage of KLRG-1<sup>high</sup> short-lived effector cells (SLECs, KLRG-1<sup>high</sup> / IL-7R $\alpha$ <sup>-</sup>) and the formation of IL-7R $\alpha$ <sup>high</sup> memory precursor cells (MPECs, KLRG-1<sup>-</sup> / IL-7R $\alpha$ <sup>+</sup>) that will give rise to memory T cells during viral infection. Once the triggering stimulus has been cleared, during the contraction phase, most of the MPECs either die, or downregulated IL-7R $\alpha$  or may be converted into SLECs. The remaining IL-7R $\alpha$ <sup>+</sup> MPECs become the source of long-lived memory cells.<sup>48,49,51</sup>

Following these premises from viral infection findings, we recreated a T cell differentiation process in a mouse model of graft vs host reaction, in which the alloreactive donor WT and CD160 KO CD8 T cell differentiation towards effector cells can be tracked down based on IL-7R $\alpha$  (CD127) and KLRG-1 surface markers along with CD27 and CD69. A couple of time points at each phase of the donor allogeneic CD8 T cell response was analyzed. Early phase of T cell activation (day 1 – day 3), clonal expansion (day 5 – day 12), effector phase (day 12 – day 17), and the contraction phase that led to the formation of long-lived memory T cell formation (day 17 – day 27) were analyzed (Fig 5A – C).

The expression of IL-7R $\alpha$  in allogeneic donor CD4 T cells (measured as MFI) fluctuated remarkably overtime. The MFI of IL-7R $\alpha$  in alloreactive donor CD4 T cells of WT and CD160 KO mice decreased significantly after the initial burst of clonal expansion compared to host F1 T cells. Then, from day 3 – day 7, IL-7R $\alpha$  expression remained low and below baseline levels. After that, it increased steeply at the onset of the effector phase reaching baseline levels at day 12 and, finally, decreased its level of expression below baseline. With respect to expression of IL-7R $\alpha$  in donor CD8 T cells, it declined significantly quickly after T cell activation up to day 5 and then kept gradually decaying its expression through day 27 (Fig 5A – B). Concerning KLRG-1 surface marker, a significant increase of the MFI was found in donor CD4 T cells and donor CD8 T cells of both WT and CD160 KO from day 12 – day 27 when compared to that of host F1 T cells. This occurred to a much greater extent in donor CD4 T cells than in donor CD8 T cells (Fig 5A – B).

The combined use of IL-7R $\alpha$  and KLRG-1 surface markers and its quasi-independent pattern of expression in effector CD8 T cells allowed us the differentiation of two effector T cell subpopulations at the peak of the response as well as at the contraction phase that precedes restoration of normal homeostasis. Accordingly, two populations of memory T cells can be distinguished: MPECs (IL-7R $\alpha$ <sup>+</sup> KLRG-1<sup>-</sup>) and SLECs (KLRG-1<sup>+</sup> IL-7R $\alpha$ <sup>-</sup>) cells. By analyzing the MPECs/SLECs ratio within the gate of donor CD8 T cells in WT compared to CD160 KO, a statistically significant difference was seen at day 12 ( $P < 0.05$ ) and day 17 ( $P < 0.005$ ) after the adoptive transfer (Fig 5B, lower panel). This finding indicates that CD160 deficiency in donor CD8 T cells affects the composition of the effector T cell pool at the effector phase of the response (Fig 5B, lower panel).

CD27 is a member of the TNFR family that interacts with CD70. Engagement of CD27 by its ligand CD70 is involved in T cell expansion and the generation of memory T cells, conferring T cells with an improved survival and cytokine secretion. Therefore, it is an essential receptor for long-term maintenance of T cell immunity. The MFI of CD27 augmented soon after the adoptive transfer of donor T cells of both CD160 WT and CD160 KO compared to host F1 T cells. This significant increase in MFI was however more prominent and long-lasting in donor CD8 T cells (from day 5 through day 27) than in donor CD4 T cells (from day 1 through day 7) in both WT and CD160 KO. Then, CD27 MFI decreased slowly in donor T cells of both WT and CD160 deficient mice approaching baseline values of host F1 T cells more rapidly in donor CD4 T cells than in donor CD8 T cells (Fig 5C).

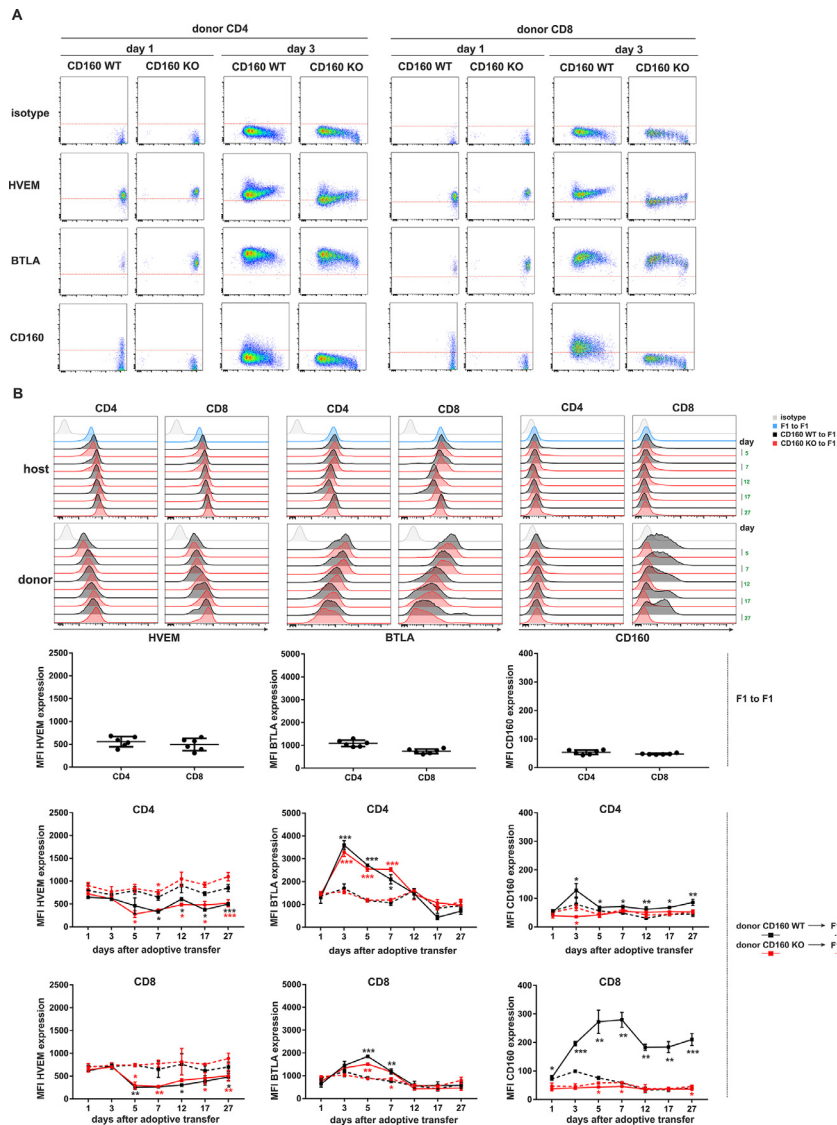


**Fig 4.** Similar dynamic of inverse regulation of HVEM and BTLA/CD160 expression in donor WT and CD160 KO T cells. (A)  $90 \times 10^6$  CFSE-labeled wild-type or CD160 deficient lymphocytes were adoptively transferred into non-irradiated CB6F1 recipients. Representative dot plots of each group showing the pattern of HVEM, and BTLA/CD160 expression in donor alloreactive CD4 T cells and donor CD8 T cells of WT and CD160 KO mice were analyzed at day 1 and day 3 after the adoptive transfer. (B, upper panel) Representative histogram plots of each molecule showing the progression of HVEM/BTLA/CD160 expression from day 5 to day 27. (B, middle panel) Baseline mean fluorescence intensity (MFI) values of HVEM/BTLA/CD160 in host F1 CD4 T cells and CD8 T cells that received syngeneic donor F1 splenocytes. (B, lower panel) The pattern of HVEM/BTLA/CD160 expression was followed along the course of the allogeneic T cell response and the MFI values for each molecule were plotted at days 1, 3, 5, 7, 12, 17 and 27 after the adoptive transfer of donor T cells to F1 recipients. These MFI values in donor T cells were compared to those MFI values in T cells of F1 hosts at each time point (black asterisks are the values of significance obtained after comparing the mean of MFI of each molecule in donor WT T cells versus mean of MFI of host F1 T cells and red asterisks compare the mean of MFI of each molecule in donor CD160 KO T cells versus the mean of MFI of host F1 T cells). Donor WT (black solid lines) to F1 host (black dotted lines) and donor CD160 KO (red solid lines) to F1 host (red dotted lines) were represented. Multiple *t*-test comparison was performed for each time point that was then corrected following the recommended Holm-Sidak correction method. *p* values were considered statistically significant according to the following criterion: \*,  $P < 0.05$ ; \*\*,  $P < 0.005$ ; \*\*\*,  $P < 0.0005$ . The plots represent the mean  $\pm$  SD of a pool of four to five mice per group and time point. HVEM, Herpesvirus entry mediator; BTLA, B- and T-lymphocyte attenuator; KO, Knock-out; MFI, Mean fluorescence intensity; WT, Wild type. For interpretation of the references to color in this figure legend, the reader is referred to the Web version of this article

Finally, CD69 (early activation antigen) MFI showed a transient and rapid increase in expression. However, by day 3 onwards, CD69 MFI values returned to baseline in donor CD4 T cells and in donor CD8 T cells of both WT and CD160 deficient mice (Fig 5C). Later on, at the end of the contraction phase, CD69 MFI values significantly increased again, although to a lower extent than at the early phase of clonal expansion in donor T cells of WT and CD160 KO mice. This reflected the condition acquired by a subpopulation of memory T cells with tissue residency preference. For this particular molecule, the absolute number of CD69 positive cells within the gate of donor CD4 T cells and donor CD8 T cells was calculated. This plot visualizes better the net and significant increase of T cells exhibiting this tissue resident memory phenotype at the end of the contraction phase of the response (Fig 5C).

In summary, these results indicate that CD160 is required for the maintenance of a proper balance of the proportion of MPECs and SLECs effector cells at the peak of the response and soon after its decline.

**CD160 deficiency did not significantly alter the alloreactive donor anti-host T cell response.** To assess the consequences of the effector phase of the allogeneic donor anti-host T cell response, the absolute number of donor CD4 T cells and donor CD8 T cells from WT or CD160 KO were analyzed overtime as well as F1 host cell counts at different time intervals from day 1 – day 27, after the adoptive transfer. Alloreactive donor WT and CD160 KO CD4 T cells clonally expanded very rapidly after T cell activation and to a similar extent, reaching the plateau of the effector phase at around day 5 – 7 and remained at plateau values until day 12. This immediate CD4 T cell response is required to provide help for the clonal expansion of CD8 T cells to drive them towards cytolytic cells. From day 12 onwards, donor CD4 T cell numbers of WT and CD160 KO contracted progressively and by day 27, they reached cell counts similar to those present at day 1 (Fig 6A, left panel).

In contrast to donor alloreactive CD4 T cells, the initiation of clonal expansion of donor CD8 T cells of WT and CD160 KO was delayed, starting at around day 7. Then, it increased steadily to reach the effector phase at day 12 (Fig 6A, right panel). At this time point, donor CD8 T cell response in both WT and CD160 KO entered the effector phase and host hematopoietic cell counts decayed rapidly due to the cytolytic attack of the donor cells leading to a profound depletion of the host hematopoiesis (Fig 6B).

In conclusion, either WT or CD160 KO allogeneic donor CD8 T cells eliminated the host hematopoietic compartment following a similar pattern of rejection.

**MHC class I mismatched skin allografts do not survive longer in CD160 KO mice than in CD160 WT mice unless CTLA-4.Ig was administered.** To dissect the role of CD160 in transplantation and graft rejection, we then took advantage of a mouse model of transplantation across an MHC class I barrier (bm1 skin grafts into B6 recipients), in which graft rejection is mediated mainly by CD8 T cells.<sup>53</sup> We found that the kinetics of allograft rejection across this MHC class I barrier was similar in CD160 WT mice and CD160 deficient mice and no significant differences were observed. Both WT and CD160 deficient mice rejected their bm1 skin allografts at around day 15 after transplantation (Fig 7). All in all, these experiments support the concept that CD160 deficiency does not impair the overall *in vivo* cytotoxic function of alloreactive CD8 T cells involved in the rejection of MHC class I mismatched allografts.

Since no major effect was detectable in this strain combination in the absence of any external therapeutic intervention, recipient mice were treated with human CTLA-4.Ig fusion protein (Abatacept, Orencia), which is cross-reactive with mouse CD80/CD86. This treatment prevents T cell costimulation by competing with CD80 and CD86 for binding to CD28, and by inducing trogocytosis of CD80 and CD86 in antigen-presenting cells.<sup>54-56</sup> This costimulation blockade intervention inhibits CD4 T cell help to CD8 T cells, which is essential for full T cell activation and further differentiation toward effector T cells. CTLA4.Ig treatment prolonged bm1 skin graft survival in WT mice ( $P < 0.05$ , \*) and in CD160 deficient mice ( $P < 0.005$ , \*\*). Furthermore, 3 out of 9 CTLA4.Ig-treated CD160 deficient mice grafted with allogeneic bm1 skin survived long-term whereas in similarly-treated WT mice, only 1 out of 11 survived up to day 60, which was the final time point recorded (Fig 7).

These findings suggest that CTLA-4.Ig treatment confers certain protection against rejection in CD160 KO mice compared to WT recipients, although the difference found did not reach statistical significance.

**Deficiency in CD160 does not impair NK cell-mediated rejection of fully MHC mismatched cellular allografts or MHC class I deficient tumor cells.** To assess whether CD160 deficiency could influence NK cell-mediated rejection of MHC mismatched cellular allografts or MHC class I deficient tumor cells, we took advantage of two experimental mouse models to evaluate *in vivo* the cytotoxic effector function of NK cells of WT and CD160 KO mice.

The differential CFSE labeling of fully MHC allogeneic cells (Balb/c) and syngeneic controls (B6) permits their distinction after *in vivo* transfer. The kinetics of rejection of the cellular allografts was followed in spleen and peripheral lymph nodes of B6 WT and B6 CD160 deficient recipients at 21, 42, and 70 hours after

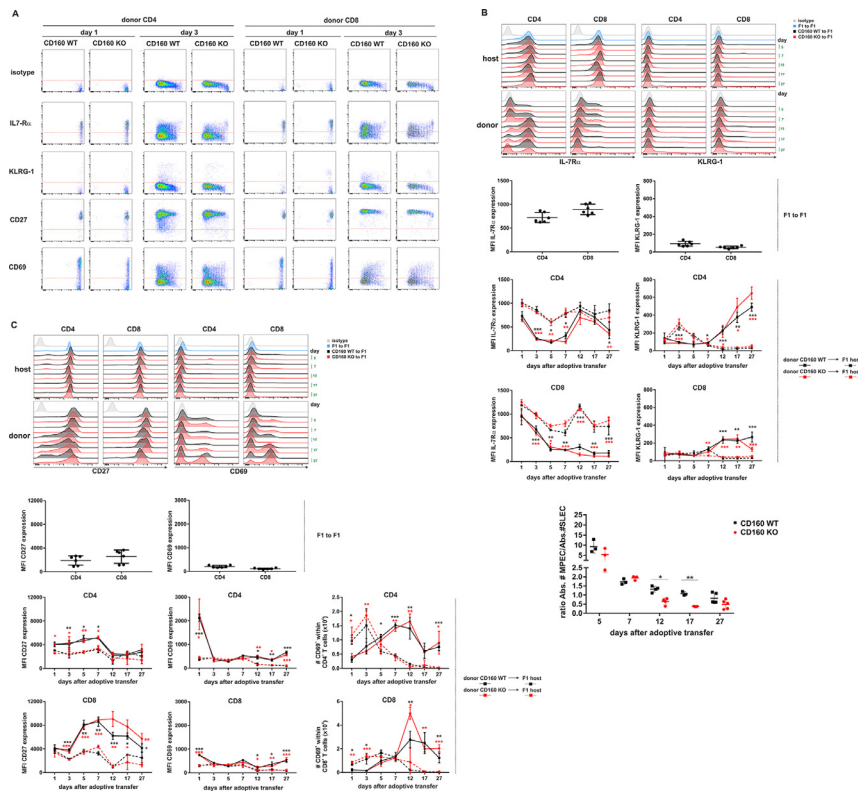


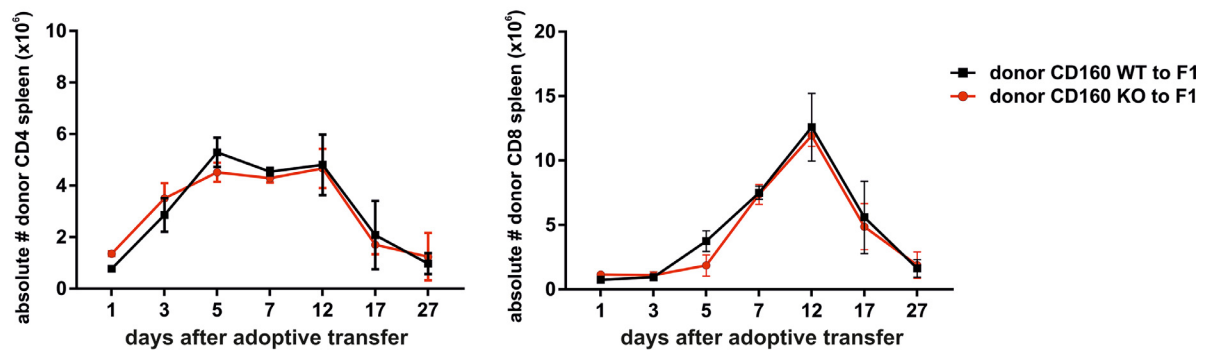
**Fig 5.** CD160 deficiency influences the normal course of T cell differentiation towards effector T cells as assessed by IL-7R $\alpha$  and KLRG-1 expression. (A) CFSE-labeled WT or CD160 KO lymphocytes were adoptively transferred into CB6F1 recipients, as described above. Representative dot plots of IL-7R $\alpha$ , KLRG-1, CD27 and CD69 expression in donor CD4 T cells and donor CD8 T cells of WT and CD160 KO collected from spleen of host F1 mice at day 1 and day 3 after the adoptive transfer. (B, upper panel) Histogram plots depict the progression of IL-7R $\alpha$  and KLRG-1 expression in host and donor WT and CD160 KO CD4 T cells and CD8 T cells (from days 5 – day 27 after the adoptive transfer) during the ascending phase of clonal expansion, effector phase and the ensuing contraction phase to return to normal homeostasis. (B, middle panel) Baseline expression of IL-7R $\alpha$  and KLRG-1 MFI values in host F1 T cells that received syngeneic donor F1 splenocytes. (B, lower panel) The pattern of IL-7R $\alpha$  and KLRG-1 expression was followed along the course of the allogeneic T cell response and the MFI values for each molecule were plotted at days 1, 3, 5, 7, 12, 17 and 27 after the adoptive transfer of donor WT or CD160 KO T cells to F1 recipients. These values were then compared to those of host F1 T cells. (B, lower panel) Follow up of the independent expression of IL-7R $\alpha$  and KLRG-1 on WT or CD160 KO donor alloreactive CD8 T cells during T cell differentiation from day 5 to day 27 after the adoptive transfer of donor lymphocytes into non-irradiated F1 recipients. The absolute number of MPECs/SLECs ratio was calculated based on IL-7R $\alpha$ /KLRG-1 expression and the results are illustrated as black squares (donor WT CD8 T cells) and red circles (donor CD160 KO CD8 T cells). (C, upper panel) Histogram graphs depict the evolution of CD27 and CD69 expression during the course of allogeneic T cell response from day 5 to day 27. (C, middle panel) Baseline of MFI values for CD27 and CD69 expression in donor CD4 T cells and donor CD8 T cells were obtained from syngeneic adoptive transfer donor F1 to host F1. (C, lower panel) The kinetic of CD27 and CD69 expression was monitored in host F1 T cells and in donor CD4 T cells and donor CD8 T cells of WT or CD160 KO overtime during T cell differentiation. Multiple *t*-test comparison was performed for each time point of the T cell differentiation process that was then corrected following the recommended Holm-Sidak correction method. Black asterisks are the values of significance obtained after comparing the mean of MFI in donor WT T cells versus mean of MFI of host F1 T cells and red asterisks compare the mean of MFI in donor CD160 KO T cells versus mean of MFI of host F1 T cells. Donor WT (black solid lines) to F1 host (black dotted lines) and donor CD160 KO (red solid lines) to F1 host (red dotted lines) were compared. The plots represent the mean  $\pm$  SD of a pool of four to five mice per group and time point. *P* values were considered statistically significant according to the following criterion: \*, *P* < 0.05; \*\*, *P* < 0.005; \*\*\*, *P* < 0.0005. CFSE, Carboxyfluorescein succinimidyl ester; KO, Knock-out; KLRG-1, glycoprotein with a C-type lectin domain and one immunoreceptor tyrosine-based inhibitory motif; IL-7R $\alpha$ , IL-7 receptor alpha; MPECs, Memory precursor effector cells; SLECs, Short-lived effector cells; WT, Wild type. For interpretation of the references to color in this figure legend, the reader is referred to the Web version of this article.

injection.<sup>57</sup> Both WT and CD160 KO NK cells killed equally well the target cells and all allogeneic Balb/c targets cells had been eliminated from the host spleen (Fig 8A) or host peripheral lymph nodes by 70 hours after the adoptive transfer (Fig 8B).

Syngeneic MHC class I deficient RMA-S tumor cells injected intraperitoneally are rapidly eliminated by an NK cell-dependent mechanism of rejection in B6

mice.<sup>45</sup> To track the tumor cells once injected i.p., both RMA control (class I sufficient) and RMA-S (class I deficient due to a defect in MHC class I assembly) syngeneic tumor cells were differentially labeled with CFSE and injected i.p. at a 1:1 ratio. The peritoneal cavity was washed by fluxing with 2mM EDTA/Glucose/D-PBS buffer and cells were collected 24 hours after injection.<sup>58,59</sup> Twenty-four

## A



## B

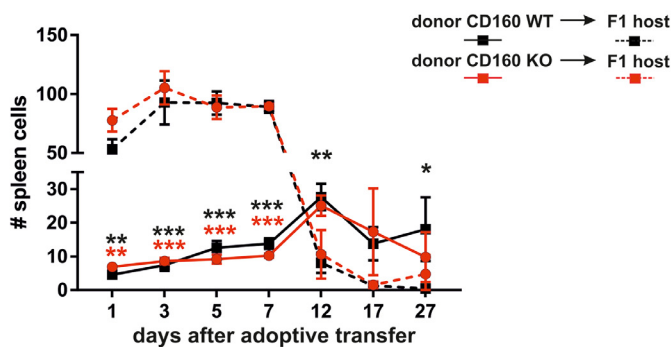


**Fig 6.** Donor anti-host reaction followed a similar kinetics in F1 recipients adoptively transferred with WT or CD160 deficient allogeneic lymphocytes. (A) The absolute number of donor allogeneic WT and CD160 KO CD4 T cells (left graph) and CD8 T cells (right graph) in the spleen was analyzed and recorded along different stages of T cell differentiation at days (1, 3, 5, 7, 12, 17, and 27) after the adoptive transfer into non-irradiated F1 recipients. (B) The absolute number of donor and host splenocytes was calculated in F1 recipients adoptively transferred with donor lymphocytes from either WT and CD160 KO along the different stages of T cell differentiation. The absolute number of splenocytes of WT and CD160 KO mice was compared to the absolute number of splenocytes of F1 hosts. Black asterisks are the values of significance obtained after comparing the absolute number of donor WT splenocytes versus the absolute number of host F1 splenocytes and red asterisks compare the absolute number of donor CD160 KO splenocytes versus absolute number of host F1 splenocytes. Donor WT splenocytes (black solid lines) to F1 host (black dotted lines) and donor CD160 KO splenocytes (red solid lines) to F1 host (red dotted lines). The plots represent the mean  $\pm$  SD of a pool of 3 to 5 mice per group and time point. *P* values were considered statistically significant according to the following criterion: \*, *P* < 0.05; \*\*, *P* < 0.005; \*\*\*, *P* < 0.0005. WT, Wild type; KO, Knock-out. For interpretation of the references to color in this figure legend, the reader is referred to the Web version of this article.

hours after i.p. implantation of tumor cells into WT or CD160 deficient mice, the peritoneal cavity cell content was examined by flow cytometry. Class I sufficient RMA tumor cells survived well without experiencing differential rejection whereas MHC class I deficient RMA-S tumor cells known to be sensitive to NK cell-mediated rejection were eliminated very efficiently to a similar extent by WT or CD160 KO NK cells (Fig 8C – D). No statistically significant differences were found between WT and CD160 KO NK cells concerning their ability to kill MHC class I deficient tumor cells.

These findings suggest that NK cell-mediated killing of allogeneic target cells or MHC class I deficient tumor cells are independent of CD160 function.

## DISCUSSION

The role of CD160 on the immune response is cell type and context-dependent and its function in distinct cell types is still a matter of intense investigation. The HVEM/CD160 signaling pathway may lead to effective or aborted lymphocyte signaling, depending upon which receptor is

activated, the phase or stage of T cell differentiation and the cellular context in which T cell activation and differentiation occurs. Both, costimulatory and coinhibitory functions have been attributed to the CD160 receptor. The majority of the evidence favors a costimulatory role for cytotoxic cells, that is, NK cells and CD8 T cells.<sup>6,16,17,20,60</sup> However, some compelling experimental data also attributed to CD160 a co-inhibitory function in NKT cells,<sup>26</sup> exhausted dysfunctional CD8 T cells,<sup>61,62</sup> and a subset of human CD4 T cells.<sup>25</sup>

In this work, the role of CD160 has been assessed on the course of allogeneic CD8 T cell cytotoxic responses in a parental to F1 GvHR model and in a skin allograft model across an MHC class I barrier. The cytotoxic response was also evaluated in a mouse model of NK cell-mediated rejection of cellular allografts across a fully MHC mismatched barrier and in an MHC class I deficient syngeneic tumor cells. We demonstrated that T cell division in both donor CD4 T cells and donor CD8 T cells of CD160 KO mice was significantly delayed compared to WT T cells during the initial phase of clonal expansion, just immediately after T cell activation in response to alloantigen stimulation. This defect in early T cell division of CD160 deficient

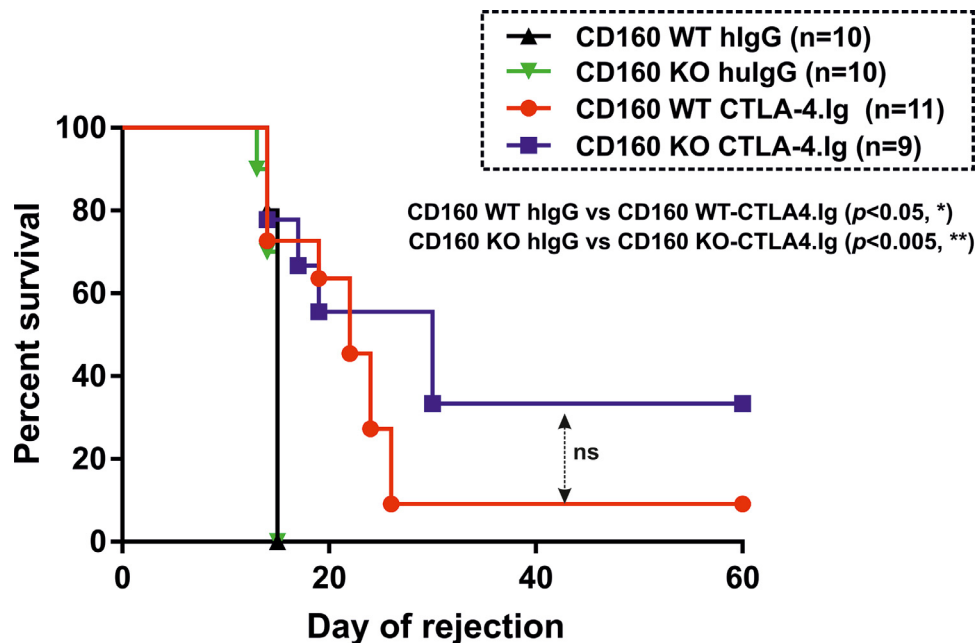


**Fig 7.** CTLA-4.Ig costimulatory blockade showed a trend of increased skin graft survival across an MHC class I mismatched barrier. Allogeneic bm1 tail skin grafts were placed on CD160 WT or CD160 KO mice, and then, mice were left untreated or were treated with control human IgG1 or human CTLA4.Ig fusion proteins (Abatacept, cross react with mouse CD80/CD86) at day 1, 7 and 14. The course of skin graft rejection was recorded overtime up to day 60. Statistical analysis to compare the survival curves was performed with the log-rank Mantel Cox test. Statistical significance is indicated as follows: \*,  $P < 0.05$ ; \*\*,  $P < 0.005$ . KO, Knock-out; CTLA4.Ig, recombinant fusion protein composed of the extracellular domain of human CTLA-4 bound to immunoglobulin. For interpretation of the references to color in this figure legend, the reader is referred to the Web version of this article.



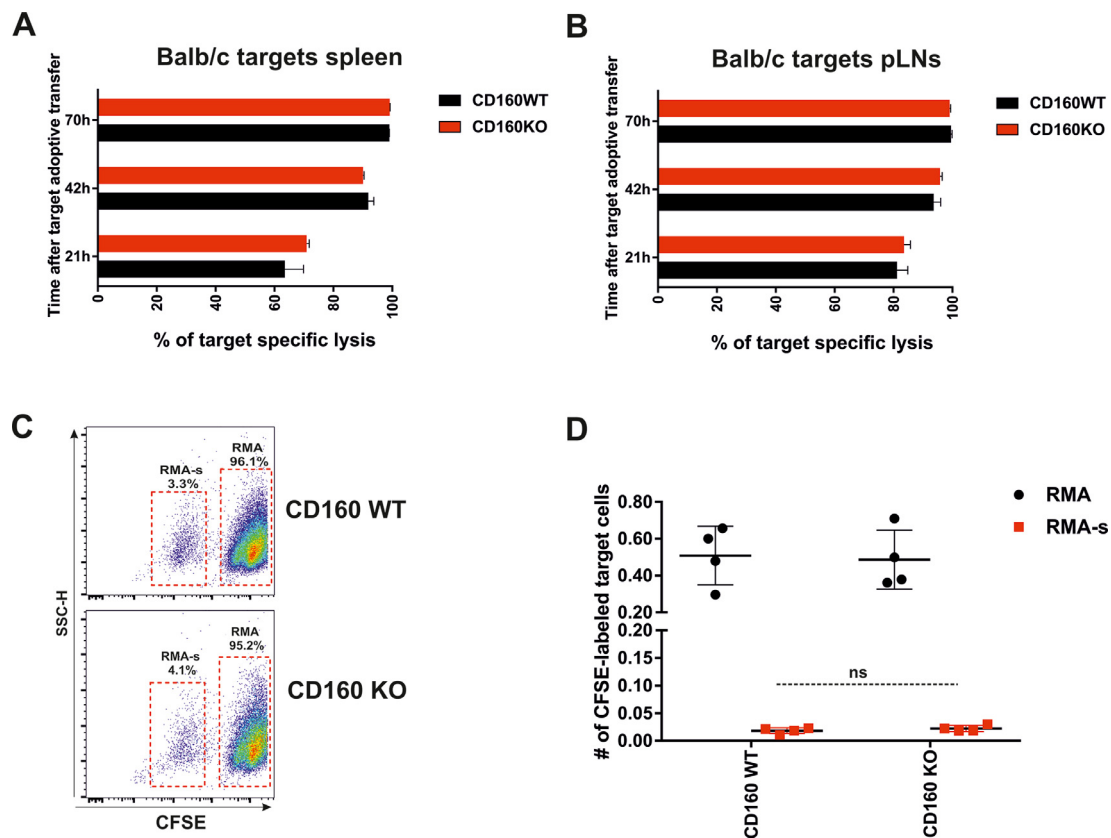


**Fig 8.** CD160 deficiency impaired neither NK cell-mediated rejection of fully MHC mismatched allogeneic cellular grafts nor rejection of MHC class I deficient syngeneic tumor cells. (A –B) Differential CFSE labeling of allogeneic Balb/c and syngeneic B6 wild-type splenocytes ( $15 \times 10^6$ ) were adoptively transferred into WT and CD160 KO mice. NK cell-mediated rejection of allogeneic cellular allografts was monitored at 21, 42 and 70 hours after the adoptive transfer in the spleen (A) and pLNs (B). The percentage of Balb/c specific lysis was calculated according to the formula described in material and methods section. The plots represent the mean  $\pm$  SD of a pool of 4 mice per group and time point. Equal numbers ( $1 \times 10^6$ ) of syngeneic CFSE-labelled RMA ( $10 \mu\text{M}$ ) (black circles) and RMA-S ( $2.5 \mu\text{M}$ ) (red squares) cells were mixed at a 1:1 ratio and injected i.p. into wild-type or CD160-deficient mice. Twenty-four hours later, peritoneal cavity lavage was performed by injecting 8 ml of EDTA/Glucose/D-PBS buffer, and the percentage (C) and the absolute number (D) of remaining non-rejected leukemia tumor cells still present in the peritoneal cavity were analyzed in both groups of mice. Student *t*-test was used for the comparison of the means. The statistical significance criteria were as follows: \*,  $P < 0.05$ ; \*\*,  $P < 0.005$ ; \*\*\*,  $P < 0.0005$ , ns: non-significant. NK, Natural killer; MHC, Major histocompatibility complex; CFSE, Carboxyfluorescein succinimidyl ester; WT, Wild type; pLNs, peripheral lymph nodes; i.p., intraperitoneal; PBS, Phosphate buffer saline. For interpretation of the references to color in this figure legend, the reader is referred to the Web version of this article.

T cells affected the course of T cell differentiation toward effector T cells. As opposed to a previous report, the absence of CD160 in NK cells did not significantly compromise its functional activity to reject cellular allografts or MHC class I deficient syngeneic leukemia tumor cells (RMA-S tumor cells) when compared to WT NK cells.<sup>27</sup>

According to a recent classification of molecules involved in co-signaling pathways, CD160 could behave as a threshold receptor for CD8 T cells and NKT cells with basal low expression at steady-state that can be upregulated upon activation under the

influence of inflammatory stimuli and remained expressed at the effector phase of the response.<sup>63</sup> This converts CD160 receptor as a very appealing target for the selective modulation of CD8 T cell-mediated allogeneic responses.

Since the discovery of CD160 by Maiza et al., (1993) and further characterized by Anumanthanin et al., (1998),<sup>15,64</sup> a compelling number of experimental evidence support the hypothesis that CD160 may represent a CD28 alternative costimulatory molecule for CD8 T cell activation. That is so in those CD8 T cells lacking CD28, recently activated CD8 T cells and

NK cells.<sup>6,16,17,23</sup> Thus, for instance, the engagement of CD160 on human T cells with soluble aggregated human MHC class I molecules (HLA-C) or anti-CD160 (clone BY55) delivers a potent proliferative signal in anti-CD3 antibody pre-activated T cells and in NK cells, but not in resting T cells.<sup>8,18-20</sup> Furthermore, soluble HVEM.Ig engagement of CD160 expressed on human NK cells enhances their cytotoxicity function and IFN- $\gamma$  secretion.<sup>17</sup>

The process of lymphocyte activation, proliferation and T cell differentiation towards effector T cells represents a current paradigm to elucidate the regulatory mechanisms involved in its control. HVEM/BTLA *cis* interaction keeps resting naïve T cells under control. Soon after T cell activation, cell membrane HVEM, BTLA and CD160 molecules undergo changes in expression. Thus, while HVEM is downregulated, BTLA and CD160 are upregulated in T cells, the latter more evident in activated CD8 T cells than in activated CD4 T cells. This permits bidirectional *trans* interaction of BTLA and CD160 that upon engaging HVEM expressed in the surrounding immune cells promotes T cell activation, proliferation, survival and cytokine secretion.<sup>21,65,66</sup> The presence of both BTLA and CD160 on the same cell such as in CD8 T cells gives CD160 a preferential ability to convey information to HVEM present in the surrounding T cells. Once CD160 is upregulated soon after CD8 T cell activation, CD160 would outcompete BTLA for binding to HVEM in *trans* favoring bidirectional exchange of information that promotes survival and costimulation of CD8 T cell responses. This is so because CD160 exhibits a slower dissociation rate than BTLA and, consequently, competes with BTLA for binding to HVEM.<sup>11</sup>

Whereas HVEM is expressed constitutively in both hematopoietic and non-hematopoietic cells, CD160 displays a pattern of expression restricted mostly to immune cells with cytotoxic activity under steady-state conditions and inflammatory conditions; however, this pattern of expression is altered soon after T cell activation in response to allogeneic stimulation. Thus, the parallel upregulation of CD160 after T cell activation and down-regulation of HVEM on the same cell may provide a window of opportunity for CD8<sup>+</sup>CD160<sup>+</sup> T cells to receive costimulatory signals from HVEM expressing cells of hematopoietic or non-hematopoietic origin. Once alloreactive donor CD8 T cells are activated, their proliferation depends on CD160 expression and its interaction in *trans* with HVEM. The mechanism that accounts for the slower proliferative activity of CD4 T cells seen in CD160 KO compared to WT counterparts is likely to be different from that of CD8 T cells because alloreactive CD4 T cells barely

increased the expression of CD160 upon activation. In this scenario, CD160 upregulation in activated alloreactive CD8 T cells may either recruit CD4 T cells into the proliferating pool by *trans* engagement of HVEM (reverse help) or indirectly through the engagement of HVEM expressed on the APC to license and enable them to convey costimulatory and survival signals to proliferating alloreactive donor CD4 T cells.

Several factors influence the outcome of CD8 T cell responses in infectious diseases. Among others, TcR signal strength, costimulation, and inflammatory cytokines released by the severity of the tissue insult (danger signals) and the replicative activity of the infectious agent. All those factors together condition the priming response and the quality and robustness of the memory recall response (long-lived memory T cells).<sup>67</sup>

Most of what we know so far on the role of HVEM/BTLA/CD160/LIGHT interaction on memory formation comes from viral infection studies performed in HVEM deficient mice, in which T cells neither receive signals through HVEM nor engage HVEM ligands (CD160, BTLA or LIGHT). The costimulatory function of HVEM on T cells is to provide survival signals and promote the conversion of effector cells into memory cells. It also imprints memory commitment on differentiating effector T cells involved in protective immunity in the mucosa in the context of bacterial and viral infections. Thus, in some viral infection models, the deficiency of HVEM in T cells has been linked to a misbalance of short-lived effector cells (SLEC) and memory precursor effector cells (MPECs).<sup>68-71</sup>

Because all these observations are coming from the study of the HVEM phenotype, an open question that still needs an answer is which HVEM interacting partner is the predominant signaling pathway that accounts for the phenotype observed in infected HVEM deficient mice. In this regard, Desai et al., found that HVEM-deficient CD8 T cells expanded normally at the early stage of T cell division, but they failed to provide survival signals to MPECs to be converted into long-lived memory T cells capable to survive long-term to sustain recall responses. They attributed this defect to the absence of HVEM/LIGHT interaction.<sup>70</sup> Other authors, for instance, Flynn et al., assigned to HVEM/BTLA bidirectional interaction a pro-survival and costimulatory function.<sup>69</sup> Muscate et al., results point in the direction that CD160 engagement on CD8 T cells by HVEM is required for the persistence of a population of terminally differentiated CD8 T cells during malaria infection.<sup>24</sup> All this evidence supports the hypothesis that apart from HVEM/LIGHT and HVEM/BTLA interaction, the engagement of CD160 by HVEM may also contribute to the survival of terminally

differentiated CD8<sup>+</sup> T cells during parasite infection. In the same line of thought are the findings of Tan et al., who demonstrated that CD160 played a costimulatory role to promote CD8 T cell effector function needed for the clearance of *Listeria* infection.<sup>16</sup>

All these findings are in line with our data that showed a rapid decay of donor CD8 T cells of MPECs phenotype (IL-7R $\alpha$ <sup>+</sup> KLRG-1<sup>-</sup> cells) in CD160 deficient donor alloreactive CD8 T cells at the onset of the effector phase when compared to donor CD8 T cell WT counterparts. Although both WT and CD160 KO donor CD8 T cells reached the minimal frequency of alloreactive T cells at the effector phase to efficiently reject an allograft, the frequency of MPECs was altered in allogeneic donor CD160 KO CD8 T cells when compared to WT donor CD8 T cells. This suggests that in the absence of intrinsic signals delivered by CD160, donor alloreactive CD8 T cells of MPECs phenotype may be prone to die by apoptosis (activation-induced cell death, AICD) or decrease in numbers due to conversion of MPECs to SLECs leading to an alteration of the MPECs/SLECs ratio at the effector phase of the response and soon after T cells enter the contraction phase.

Apart from the differences observed in T cell expansion rate after T cell activation in donor CD160 deficient T cells compared to WT T cells and the change in the composition of effector cells at the peak of the response and soon after, donor T cells from WT and CD160 KO mice behave similarly in terms of the kinetic of rejection and modulation of expression of the set of molecules studied.

Our study showed that CD160 deficient NK cells killed MHC class I deficient leukemia RMA-S tumor cells with the same efficiency as WT NK cells did, while Tu et al., found a defect in NK cell-mediated killing of RMA-S class I deficient tumor cells.<sup>27</sup> To reconcile these apparently discrepant results, one fact that may account for this difference is that Tu et al., implanted RMA-S tumor cells subcutaneously instead of implanting them into the peritoneal cavity. Subcutaneous implantation of the tumor limits tumor progression due to unfitting microenvironment, whereas in the peritoneal cavity model of tumor implantation, tumor cells are in suspension, and there, they are much more exposed to direct contact, and subsequent killing by resident NK cells.

In summary, our findings suggest that CD160 may function as a CD28 alternative costimulatory molecule, which is upregulated upon T cell activation and displays a pattern of expression restricted to cytotoxic T cells being important for proper CD8 T cell differentiation towards effector T cells and memory T cells. This work supports an immunoregulatory role of CD160 in transplantation that can be leveraged in combination with costimulation blockade to achieve a better control of allogeneic CD8 T cell responses involved in graft rejection.

## ACKNOWLEDGEMENTS

**Conflict of Interest:** The authors declare no conflict of interest. All authors have read the journal's policy on conflicts of interest and have no conflicts of interest to disclose. All authors have read the journal's authorship agreement and confirm that the manuscript has been reviewed and approved by all named authors.

This work has been supported by grants of the Spanish Ministry of Science and Universities (Grant # [PID2019-103984RB-I00](#)), Department of Education of Castilla and Leon Regional Government (Grant # [LE-006P20](#)) to JIRB and it was also partially funded by the Spanish Network of Cancer Research, Ciberonc (Grant # [CB16/12/00480](#)). This work was partially financially supported by the “TEFOR” project funded by the “Investissements d’Avenir” French Government program, managed by the French National Research Agency (ANR) (ANR11-INSB-0014) and by the IHU-Cesti project (ANR-10-IBHU-005) which is part of the “Investissements d’Avenir” French Government program managed by the ANR. The IHU-Cesti project is also supported by Nantes Métropole and Région Pays de la Loire.

**Author contributions:** M.L.R. and J.I.R.B. designed the study, performed and analyzed the experiments and wrote the manuscript. T.H.N, L.S, J.M.H. and I.A. contributed to the CRISPR/Cas9 targeting strategy; A.G. A, R.F.G and J.G.A. were involved in the microinjection into zygotes; J.A.P.S and L.B. contributed with reagents and their expertise in the field. All authors contributed to the final version of the manuscript.

## SUPPLEMENTARY MATERIALS

Supplementary material associated with this article can be found in the online version at doi:[10.1016/j.trsl.2021.08.006](https://doi.org/10.1016/j.trsl.2021.08.006).

## REFERENCES

1. Ford ML. T Cell cosignaling molecules in transplantation. *Immunity* 2016;44:1020–33.
2. Wang S, Chen L. T lymphocyte co-signaling pathways of the B7-CD28 family. *Cell Mol Immunol* 2004;1:37–42.
3. Bodmer JL, Schneider P, Tschopp J. The molecular architecture of the TNF superfamily. *Trends Biochem Sci* 2002;27:19–26.
4. Yokoyama WM, Daniels BF, Seaman WE, Hunziker R, Margulies DH, Smith HR. A family of murine NK cell receptors specific for target cell MHC class I molecules. *Semin Immunol* 1995;7:89–101.
5. Maeda M, Carpenito C, Russell RC, et al. Murine CD160, Ig-like receptor on NK cells and NKT cells, recognizes classical and nonclassical MHC class I and regulates NK cell activation. *J Immunol* 2005;175:4426–32.
6. Le Bouteiller P, Tabiasco J, Polgar B, et al. CD160: A unique activating NK cell receptor. *Immunol Lett* 2011;138:93–6.

7. Giustiniani J, Bensussan A, Marie-Cardine A. Identification and characterization of a transmembrane isoform of CD160 (CD160-TM), a unique activating receptor selectively expressed upon human NK cell activation. *J Immunol* 2009;182:63–71.
8. Barakonyi A, Rabot M, Marie-Cardine A, et al. Cutting edge: engagement of CD160 by its HLA-C physiological ligand triggers a unique cytokine profile secretion in the cytotoxic peripheral blood NK cell subset. *J Immunol* 2004;173:5349–54.
9. Giustiniani J, Marie-Cardine A, Bensussan A. A soluble form of the MHC class I-specific CD160 receptor is released from human activated NK lymphocytes and inhibits cell-mediated cytotoxicity. *J Immunol* 2007;178:1293–300.
10. Cai G, Freeman GJ. The CD160, BTLA, LIGHT/HVEM pathway: a bidirectional switch regulating T-cell activation. *Immunol Rev* 2009;229:244–58.
11. Kojima R, Kajikawa M, Shiroishi M, Kuroki K, Maenaka K. Molecular basis for herpesvirus entry mediator recognition by the human immune inhibitory receptor CD160 and its relationship to the cosignaling molecules BTLA and LIGHT. *J Mol Biol* 2011;413:762–72.
12. Liu W, Garrett SC, Fedorov EV, et al. Structural Basis of CD160:HVEM recognition. *Structure (London, England : 1993)* 2019;27:1286–95, e4.
13. Tsujimura K, Obata Y, Matsudaira Y, et al. Characterization of murine CD160+ CD8+ T lymphocytes. *Immunol Lett* 2006;106:48–56.
14. Del Rio ML, Bravo Moral AM, Fernandez-Renedo C, et al. Modulation of cytotoxic responses by targeting CD160 prolongs skin graft survival across major histocompatibility class I barrier. *Transl Res* 2017;181:83–95, e3.
15. Anumanthan A, Bensussan A, Boumsell L, et al. Cloning of BY55, a novel Ig superfamily member expressed on NK cells, CTL, and intestinal intraepithelial lymphocytes. *J Immunol* 1998;161:2780–90.
16. Tan CL, Peluso MJ, Drijvers JM, et al. CD160 Stimulates CD8(+) T Cell responses and is required for optimal protective immunity to listeria monocytogenes. *Immuno Horizons* 2018;2:238–50.
17. Sedy JR, Bjordahl RL, Bekiaris V, Macauley MG, Ware BC, Norris PS, et al. CD160 activation by herpesvirus entry mediator augments inflammatory cytokine production and cytolytic function by NK cells. *J Immunol (Baltimore, Md : 1950)* 2013;191:828–36.
18. Nikolova M, Marie-Cardine A, Boumsell L, Bensussan A. BY55/CD160 acts as a co-receptor in TCR signal transduction of a human circulating cytotoxic effector T lymphocyte subset lacking CD28 expression. *Int Immunol* 2002;14:445–51.
19. Agrawal S, Marquet J, Freeman GJ, et al. Cutting edge: MHC class I triggering by a novel cell surface ligand costimulates proliferation of activated human T cells. *J Immunol* 1999;162:1223–6.
20. Le Bouteiller P, Barakonyi A, Giustiniani J, et al. Engagement of CD160 receptor by HLA-C is a triggering mechanism used by circulating natural killer (NK) cells to mediate cytotoxicity. *Proc Natl Acad Sci USA* 2002;99:16963–8.
21. Cheung TC, Steinberg MW, Osborne LM, et al. Unconventional ligand activation of herpesvirus entry mediator signals cell survival. *Proc Natl Acad Sci USA* 2009;106:6244–9.
22. Shui JW, Larange A, Kim G, et al. HVEM signalling at mucosal barriers provides host defence against pathogenic bacteria. *Nature* 2012;488:222–5.
23. Zhang L, Zhang A, Xu J, et al. CD160 plays a protective role during chronic infection by enhancing both functionalities and proliferative capacity of CD8+ T Cells. *Front Immunol* 2020;11:2188.
24. Muscate F, Stetter N, Schramm C, Schulze Zur Wiesch J, Bosurgi L, Jacobs T. HVEM and CD160: regulators of immunopathology during malaria blood-stage. *Front Immunol* 2018;9:2611.
25. Cai G, Anumanthan A, Brown JA, Greenfield EA, Zhu B, Freeman GJ. CD160 inhibits activation of human CD4+ T cells through interaction with herpesvirus entry mediator. *Nat Immunol* 2008;9:176–85.
26. Kim TJP, G.; Kim, J.; Lim, S.A.; et al. CD160 serves as a negative regulator of NKT cells in acute hepatic injury. *Nature communications*. 2019;10:3258.
27. Tu TC, Brown NK, Kim TJ, et al. CD160 is essential for NK-mediated IFN-gamma production. *J Exp Med* 2015;212:415–29.
28. Remy S, Chenouard V, Tesson L, et al. Generation of gene-edited rats by delivery of CRISPR/Cas9 protein and donor DNA into intact zygotes using electroporation. *Sci Rep* 2017;7:16554.
29. Mojica FJ, Diez-Villasenor C, Garcia-Martinez J, Soria E. Intervening sequences of regularly spaced prokaryotic repeats derive from foreign genetic elements. *J Mol Evol* 2005;60:174–82.
30. Doudna JA, Charpentier E. Genome editing. The new frontier of genome engineering with CRISPR-Cas9. *Science* 2014;346:1258096.
31. Cong L, Zhang F. Genome engineering using CRISPR-Cas9 system. *Methods Mol Biol* 2015;1239:197–217.
32. Komor AC, Badran AH, Liu DR. CRISPR-based technologies for the manipulation of eukaryotic genomes. *Cell* 2016;168:20–36.
33. Gómez-Redondo I, Ramos-Ibeas P, Pericuesta E, Fernández-González R, Laguna-Barraza R, Gutiérrez-Adán A. Minor splicing factors Zrsr1 and Zrsr2 are essential for early embryo development and 2-Cell-like conversion. *Int J Mol Sci* 2020;21:4115–30.
34. Ran FA, Hsu PD, Wright J, Agarwala V, Scott DA, Zhang F. Genome engineering using the CRISPR-Cas9 system. *Nat Protoc* 2013;8:2281–308.
35. Vouillot L, Thelie A, Pollet N. Comparison of T7E1 and surveyor mismatch cleavage assays to detect mutations triggered by engineered nucleases. *G3 (Bethesda, Md)* 2015;5:407–15.
36. Horiuchi K, Perez-Cerezales S, Papisaikas P, et al. Impaired spermatogenesis, muscle, and erythrocyte function in U12 intron splicing-defective Zrsr1 Mutant Mice. *Cell Rep* 2018;23:143–55.
37. Fernández-González R, Laguna R, Ramos-Ibeas P, et al. Successful ICSI in mice using caput epididymal spermatozoa. *Front Cell Dev Biol* 2019;7:346.
38. Unkeless JC. Characterization of a monoclonal antibody directed against mouse macrophage and lymphocyte Fc receptors. *J Exp Med* 1979;150:580–96.
39. Kumar V, George T, Yu YY, Liu J, Bennett M. Role of murine NK cells and their receptors in hybrid resistance. *Curr Opin Immunol* 1997;9:52–6.
40. Pulaiev RA, Pulaieva IA, Ryan AE, Via CS. The Parent-into-F1 Model of Graft-vs-Host Disease as a Model of In Vivo T Cell Function and Immunomodulation. *Curr Med Chem Immunol Endocr Metab Agents* 2005;5:575–83.
41. Lyons AB. Analysing cell division in vivo and in vitro using flow cytometric measurement of CFSE dye dilution. *J Immunol Methods* 2000;243:147–54.
42. Suchin EJ, Langmuir PB, Palmer E, Sayegh MH, Wells AD, Turka LA. Quantifying the frequency of alloreactive T cells in vivo: new answers to an old question. *J Immunol (Baltimore, Md : 1950)* 2001;166:973–81.
43. Rodriguez-Barbosa JI, Ferreras MC, Buhler L, et al. Therapeutic implications of NK cell regulation of allogeneic CD8 T cell-mediated immune responses stimulated through the direct pathway of antigen presentation in transplantation. *mAbs* 2018;10:1030–44.
44. del Rio ML, Kaye J, Rodriguez-Barbosa JI. Detection of protein on BTLA(low) cells and in vivo antibody-mediated down-modulation

- of BTLA on lymphoid and myeloid cells of C57BL/6 and BALB/c BTLA allelic variants. *Immunobiology* 2010;215:570–8.
45. Smyth MJ, Kelly JM, Baxter AG, Korner H, Sedgwick JD. An essential role for tumor necrosis factor in natural killer cell-mediated tumor rejection in the peritoneum. *J Exp Med* 1998;188:1611–9.
  46. Thierry-Mieg D, Thierry-Mieg J. AceView: a comprehensive cDNA-supported gene and transcripts annotation. *Genome Biol* 2006;7(Suppl 1):S121–4.
  47. Song HK, Noorchashm H, Lieu YK, et al. Tracking alloreactive cell division in vivo. *Transplantation* 1999;68:297–9.
  48. Kaech SM, Tan JT, Wherry EJ, Konieczny BT, Surh CD, Ahmed R. Selective expression of the interleukin 7 receptor identifies effector CD8 T cells that give rise to long-lived memory cells. *Nat Immunol* 2003;4:1191–8.
  49. Ferrer IR, Wagener ME, Song M, Ford ML. CD154 blockade alters innate immune cell recruitment and programs alloreactive CD8+ T cells into KLRG-1(high) short-lived effector T cells. *PLoS One* 2012;7:e40559.
  50. Bozeman AM, Laurie SJ, Haridas D, Wagener ME, Ford ML. Transplantation preferentially induces a KLRG-1(lo) CD127(hi) differentiation program in antigen-specific CD8(+) T cells. *Transpl Immunol* 2018;50:34–42.
  51. Sarkar S, Kalia V, Haining WN, Konieczny BT, Subramaniam S, Ahmed R. Functional and genomic profiling of effector CD8 T cell subsets with distinct memory fates. *J Exp Med* 2008;205:625–40.
  52. Remmerswaal EBM, Hombrink P, Nota B, Pircher H, Ten Berge IJM, van Lier RAW, et al. Expression of IL-7R $\alpha$  and KLRG1 defines functionally distinct CD8(+) T-cell populations in humans. *Eur J Immunol* 2019;49:694–708.
  53. Auchincloss H Jr., Mayer T, Ghobrial R, Winn HJ. T-cell subsets, bm mutants, and the mechanisms of allogeneic skin graft rejection. *Immunol Res* 1989;8:149–64.
  54. Wekerle T, Grinyo JM. Belatacept: from rational design to clinical application. *Transpl Int* 2012;25:139–50.
  55. Qureshi OS, Zheng Y, Nakamura K, et al. Trans-endocytosis of CD80 and CD86: a molecular basis for the cell-extrinsic function of CTLA-4. *Science* 2011;332:600–3.
  56. Salomon B, Bluestone JA. Complexities of CD28/B7: CTLA-4 costimulatory pathways in autoimmunity and transplantation. *Annu Rev Immunol* 2001;19:225–52.
  57. Brehm MA, Daniels KA, Ortaldo JR, Welsh RM. Rapid conversion of effector mechanisms from NK to T cells during virus-induced lysis of allogeneic implants in vivo. *J Immunol* 2005;174:6663–71.
  58. Saudemont A, Burke S, Colucci F. A simple method to measure NK cell cytotoxicity in vivo. *Methods Mol Biol* 2010;612:325–34.
  59. Karre K, Ljunggren HG, Piontek G, Kiessling R. Selective rejection of H-2-deficient lymphoma variants suggests alternative immune defence strategy. *Nature* 1986;319:675–8.
  60. Rodriguez-Barbosa JI, Schneider P, Weigert A, Lee KM, Kim TJ, Perez-Simon JA, et al. HVEM, a cosignaling molecular switch, and its interactions with BTLA, CD160 and LIGHT. *Cell Mol Immunol* 2019;16:679–82.
  61. Viganò S, Banga R, Bellanger F, Pellaton C, Farina A, Comte D, et al. CD160-associated CD8 T-cell functional impairment is independent of PD-1 expression. *PLoS Pathog* 2014;10:e1004380.
  62. Blackburn SD, Shin H, Haining WN, Zou T, Workman CJ, Polley A, et al. Coregulation of CD8+ T cell exhaustion by multiple inhibitory receptors during chronic viral infection. *Nat Immunol* 2009;10:29–37.
  63. Rumpert M, Drylewicz J, Ackermans LJE, Borghans JAM, Medzhitov R, Meyaard L. Functional categories of immune inhibitory receptors. *Nat Rev Immunol* 2020;20:771–80.
  64. Maiza H, Leca G, Mansur IG, Schiavon V, Boumsell L, Bensussan A. A novel 80-kD cell surface structure identifies human circulating lymphocytes with natural killer activity. *J Exp Med* 1993;178:1121–6.
  65. Del Rio ML, Jones ND, Buhler L, et al. Selective blockade of herpesvirus entry mediator-B and T lymphocyte attenuator pathway ameliorates acute graft-versus-host reaction. *J Immunol* 2012;188:4885–96.
  66. Del Rio ML, Schneider P, Fernandez-Renedo C, Perez-Simon JA, Rodriguez-Barbosa JI. LIGHT/HVEM/LTbetaR interaction as a target for the modulation of the allogeneic immune response in transplantation. *Am J Transplant* 2013;13:541–51.
  67. Masopust D, Schenkel JM. The integration of T cell migration, differentiation and function. *Nat Rev Immunol* 2013;13:309–20.
  68. Steinberg MW, Huang Y, Wang-Zhu Y, Ware CF, Cheroutre H, Kronenberg M. BTLA interaction with HVEM expressed on CD8(+) T cells promotes survival and memory generation in response to a bacterial infection. *PLoS One* 2013;8:e77992.
  69. Flynn R, Hutchinson T, Murphy KM, Ware CF, Croft M, Salek-Ardakani S. CD8 T cell memory to a viral pathogen requires trans cosignaling between HVEM and BTLA. *PLoS One* 2013;8:e77991.
  70. Desai P, Abboud G, Stanfield J, et al. HVEM Imprints memory potential on effector CD8 T cells required for protective mucosal immunity. *J Immunol (Baltimore, Md : 1950)* 2017;199:2968–75.
  71. Park SJ, Riccio RE, Kopp SJ, Ifergan I, Miller SD, Longnecker R. Herpesvirus entry mediator binding partners mediate immunopathogenesis of ocular herpes simplex virus 1 infection. *mBio* 2020;11:e00790-20.
  72. Del Rio ML, Fernandez-Renedo C, Chaloin O, et al. Immunotherapeutic targeting of LIGHT/LTbetaR/HVEM pathway fully recapitulates the reduced cytotoxic phenotype of LIGHT-deficient T cells. *mAbs* 2016;8:1–13.